Hydrogeology Journal (2020) 28:1593–1613
https://doi.org/10.1007/s10040-020-02193-z

REPORT

Rethinking groundwater flow on the South Rim of the Grand Canyon, USA: characterizing recharge sources and flow paths with environmental tracers

John E. Solder[1] · Kimberly R. Beisner[2] · Jessica Anderson[3] · Don J. Bills[3]

Received: 20 August 2019 / Accepted: 23 May 2020 / Published online: 30 June 2020

Abstract

In the arid landscape south of the Grand Canyon, natural springs and seeps are a critical resource for endemic species and Native American tribes. Groundwater is potentially threatened by expanding populations, tourism, and mineral extraction activities. Environmental tracers, including noble gases, stable isotopes of hydrogen and oxygen in water, tritium, and carbon-14, were used to characterize recharge sources and flow paths in South Rim aquifers. Results confirm the regional Redwall-Muav aquifer is the primary groundwater source to springs. However, a second local recharge source is required to explain the detection of tritium. Probable sources are: (1) low-elevation infiltration of surface run-off with warm recharge temperatures and high excess air determined from noble gas models, and relatively low fractions of winter recharge, and (2) high-elevation plateau recharge with cool recharge temperatures, low excess air, and fraction of winter recharge of approximately 1. Previous investigators have linked spring occurrence with regional faults and fractures. Such features also likely control the chemical mixing between the regional and local groundwater sources, the transport of deeply sourced and local recharge fluids, groundwater age, and thus the relative vulnerability of groundwater to depletion and contamination. The new conceptual model of groundwater sources and flow paths suggests that many South Rim springs may respond on the order of tens to hundreds of years to groundwater depletion and contamination, even though the majority of groundwater flow is along longer flow paths with longer lag times. The magnitude of response to short-term changes in the flow system remains unclear.

Keywords USA · Water-resources conservation · Groundwater age · Radioactive isotopes · Noble gas

Introduction

Protecting ecologically, culturally, and economically important springs, seeps, and streams along the South Rim of Grand Canyon National Park (GRCA) are priorities for the National Park Service and the Havasupai Tribe. Located in the desert environment of northern Arizona (USA), springs on the South Rim are critical resources for diverse native ecology, for Native Americans as a water supply and sacred sites (Stevens and Meretsky 2008), and for the local economy. Along the South Rim, human habitation is almost entirely dependent on groundwater. GRCA tourism has rapidly increased to over 6.25 million park visits in 2017 (National Park Service 2018). Most water used at park facilities originates from the North Rim springs, but other water sources are needed and are being developed to meet the park service's projected needs. Ongoing residential expansion in the towns of Williams, Valle, and Tusayan also relies on groundwater wells (Fig. 1; Montgomery and Associates 1999) further stressing the system. Over 42,000 visitors per year explore the inner canyon on overnight trips (Sullivan 2018) where spring resources are a critical water supply. Additional visitors that

Electronic supplementary material The online version of this article (https://doi.org/10.1007/s10040-020-02193-z) contains supplementary material, which is available to authorized users.

✉ John E. Solder
jsolder@usgs.gov

[1] US Geological Survey, Utah Water Science Center, 2329 W. Orton Cir., Salt Lake City, UT 84119, USA

[2] US Geological Survey, New Mexico Water Science Center, 6700 Edith Blvd. NE, Albuquerque, NM 87113, USA

[3] US Geological Survey, Arizona Water Science Center, 2255 N. Gemini Dr., Flagstaff, AZ 86001, USA

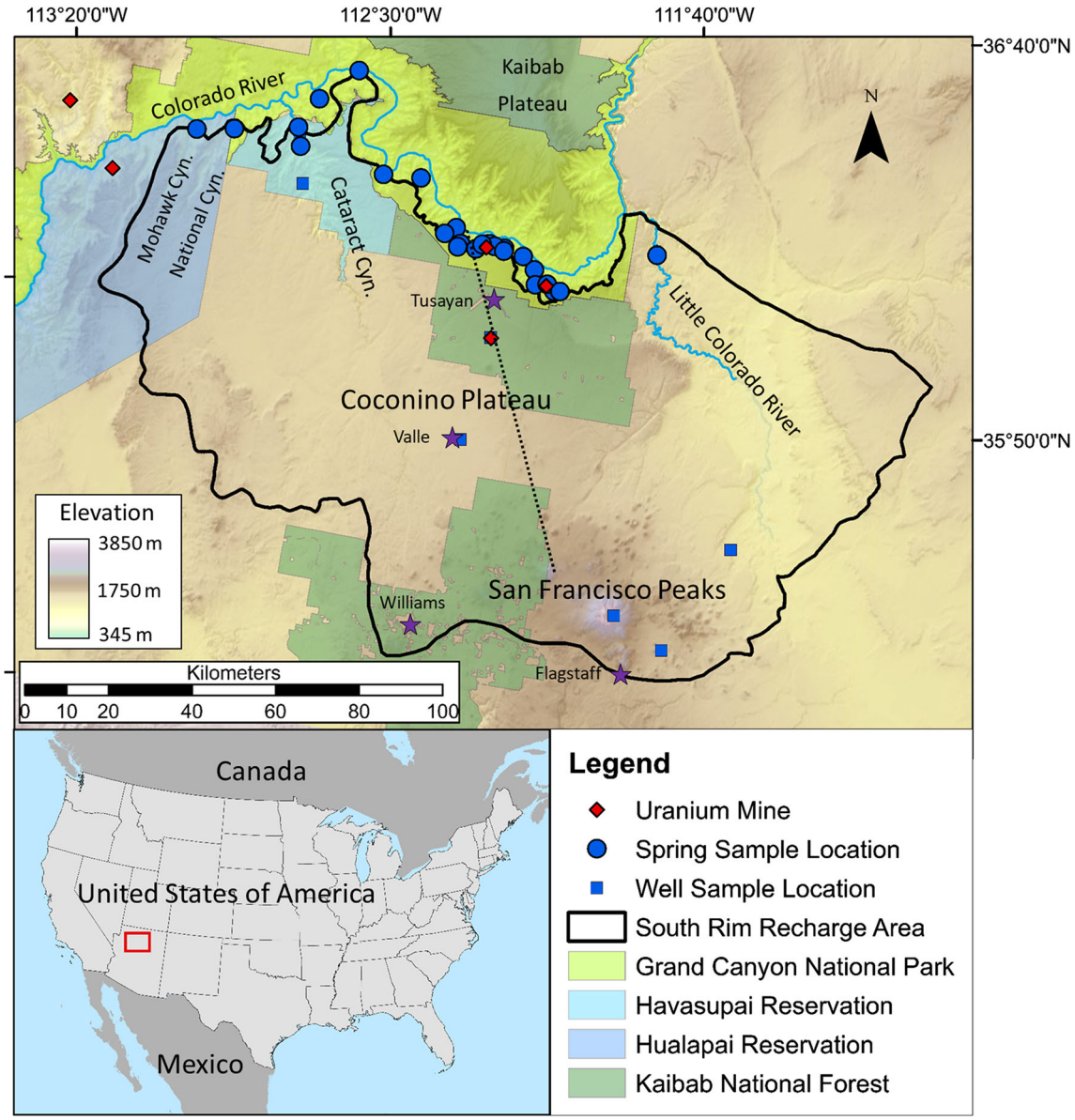

Fig. 1 Map of study area indicating potential recharge area (black border), municipalities (purple stars), major streams and rivers (blue lines), major geographical features (black text), and location of cross-section shown in the subsequent figure (dotted line). Land surface elevation relative to NAVD88 indicated by shading from ~350 m (green) to ~3,900 m (white) from US Geological Survey (2016)

access springs outside GRCA boundaries such as the iconic blue-green streams and waterfalls of Havasu Spring on Havasupai Tribal lands, provide a vital source of income.

Groundwater development is superimposed on the decades-long dry cycle across the Southwest USA (McCabe et al. 2004; MacDonald et al. 2008) with even more pronounced impacts of reduced precipitation and recharge in northern Arizona (Hereford et al. 2014). The combined factors of drought and development have already reduced, or in some instances stopped, groundwater flow from South Rim springs and flow to shallow springs and wells between Flagstaff and Williams (Bills et al. 2007). Additional withdrawal of groundwater from the regional aquifer systems will further reduce flows and might alter the water quality within GRCA and adjacent reservation lands (Tobin et al. 2017). Understanding the source and pathways of groundwater transport to South Rim springs is vital for responsible stewardship of these groundwater-dependent resources.

The primary concern for groundwater quality is the release of heavy metals such as uranium from abandoned and active breccia pipe uranium mines within the study area (Fig. 1; Alpine 2010). While on-going study aims to establish the trace element concentrations that occur naturally (see Beisner and Tillman 2018, and Beisner et al. 2020), previous investigators have noted that mining activity has probably accelerated

erosion of some of these uranium deposits (Alpine 2010). Studies by the US Geological Survey (USGS) aim to better understand the potential groundwater impacts from legacy and future uranium mining activity on the South and North Rims (e.g., this work; 2010; Beisner et al. 2017a, b, 2020; Beisner and Tillman 2018; Solder and Beisner 2020). The continued availability of high-quality groundwater along the South Rim depends on better understanding of the source and flow paths of groundwater in the area.

This report focuses on the South Rim of the Grand Canyon between the Little Colorado River and National Canyon (Fig. 1), known to contain hundreds of groundwater-fed springs, seeps, and stream resources. Environmental age tracers (tritium and carbon-14) and dissolved noble gases (He, Ne, Ar, Xe, Kr) from 12 springs and 2 wells are used to characterize groundwater age and recharge source(s). Age tracer data from an additional 19 springs and wells were compiled from earlier investigations to supplement newly collected data. Multi-tracer methods have been successfully used to investigate karst systems with high-elevation recharge inputs (e.g., Land and Huff 2010; Gardner and Heilweil 2014; Land and Timmons 2016; Han et al. 2017; Lerback et al. 2019) and provide unique insights on system functioning. Two companion studies (Solder and Beisner 2020; Beisner et al. 2020)—one that develops a stable isotope mixing model for identifying recharge sources and the other that presents detailed geochemistry to further characterize water–rock interaction in the groundwater flow system—are associated with this work. The combined studies provide the most comprehensive characterization of South Rim groundwater to date. This report makes use of a broad suite of hydrologic tracers to identify (1) groundwater recharge sources and mechanisms, (2) sources of elevated helium concentrations in groundwater, (3) controls on groundwater age and tracer chemistry, and (4) controls on groundwater flow paths.

Materials and methods

Study area

Grand Canyon National Park is located in northwestern Arizona on the southern Colorado Plateau (Fig. 1; Hunt 1967). Within the study area, elevation of the Grand Canyon ranges from 530 m relative the North American Vertical Datum of 1988 (NAVD88) at the mouth of National Canyon to 2,280 m at the South Rim near Grandview Point. Elevations south of the canyon range between 1,700 and 2,300 m on the Coconino Plateau up to 3,850 m on Humphreys Peak, the tallest point on the San Francisco Peaks volcanic field. The climate is semiarid to arid with spatial and temporal extremes of temperature and precipitation. Immediate to the canyon, annual precipitation ranges between 152 mm along the river at the eastern end of GRCA to 406 mm at the South Rim (WRCC 2018) with some of the largest single precipitation events occurring as localized summer thunderstorms. Annual precipitation near the southwestern base of San Francisco Peaks is 600 mm (USC00023009 30-year Normal 1981-2010; NOAA 2018); higher elevations likely experience even greater amounts of precipitation. Average annual temperatures range from about 15.5 °C on the South Rim to about 26.6 °C at the canyon's bottom. Summer temperatures commonly exceed 37.7 °C on the Coconino Plateau and reach 43.3–48.9 °C in the inner canyons (WRCC 2018). Average annual evaporation rates are large, more than 20 times the average annual precipitation for much of the area (Farnsworth et al. 1982), resulting in a net annual water deficit for most of northern Arizona. Water is present, as limited surface-water bodies and groundwater, because most of the precipitation falls in the winter months when evaporation processes are at a minimum or during intense localized summer thunderstorms.

Hydrogeologic conceptualization

The simple layered geology exposed in the Grand Canyon Region obscures the complex character of the perched and regional groundwater-flow systems. The geology and structure of the study area has been mapped by Billingsley and Hampton (2000), Billingsley et al. (2006, 2007), and Haynes and Hackman (1978). The Coconino and Redwall-Muav aquifers are the two principal groundwater flow systems on the Coconino Plateau (Fig. 2; Metzger 1961; Hart et al. 2002; Bills et al. 2007). The majority of South Rim springs discharge from the Redwall-Muav aquifer. A minor aquifer is present in the underlying Proterozoic rock (Metzger 1961; Cooley 1976). Understanding the occurrence and movement of groundwater in the Coconino and Redwall-Muav aquifers is limited by complex structural geology and a lack of data from wells intercepting the aquifers. Regional fractures and faults act both as barriers and preferential pathways for horizontal and vertical groundwater movement (Huntoon 1977) and are also associated with the development of karst conduits (Huntoon 1977, 2000). Springs are often present where fractures and faults intersect the canyon (Huntoon 1977; Brown and Moran 1979).

The Coconino aquifer is a relatively shallow unconfined system consisting of hydraulically connected sandstones and limestones of the Coconino Sandstone, Toroweap Formation, and the Kaibab Formation (Fig. 2). Coarse-grained portions of the upper and middle Supai Group can also be considered part of the Coconino aquifer depending on lateral continuity of shales (Bills et al. 2007). The Hermit Formation at the base of the Coconino Sandstone and the fine-grained units lower in the Supai Group act as aquitards, although faults and fractures potentially allow groundwater flow through these units.

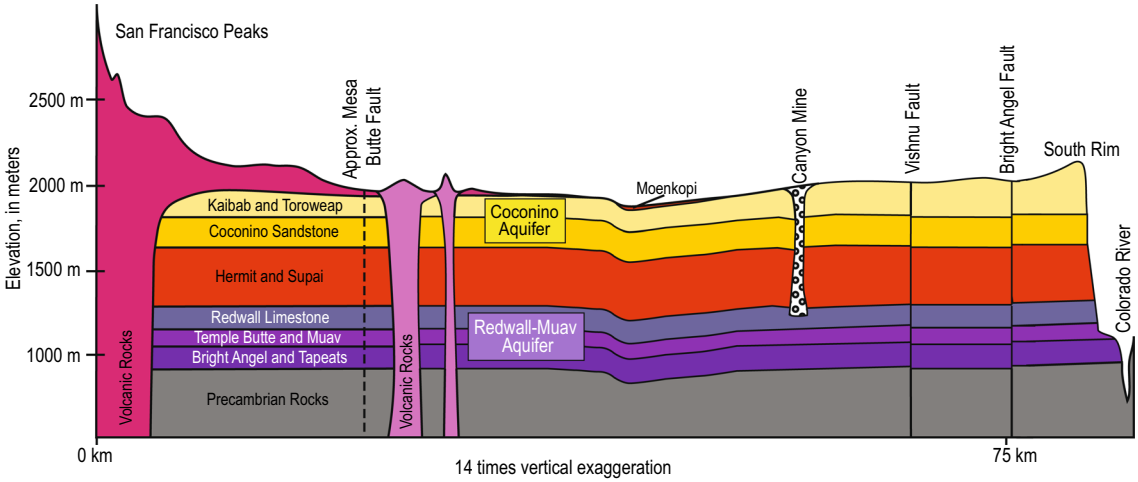

Fig. 2 Conceptual hydrogeology of the South Rim, Grand Canyon, USA. Primary hydrogeologic units, groundwater flow systems, and geographic features (black text) indicated. Figure modified from Beisner et al. (2020).

Focused recharge to the Coconino aquifer likely occurs along the San Francisco Peaks mountain front and at collapse features (i.e., breccia pipes; Hart et al. 2002; Monroe et al. 2005; Bills et al. 2007; Tobin et al. 2017) and alluvial channel bottoms on the Coconino Plateau (USDA 1986). Areally diffuse recharge from direct precipitation and snowmelt on the Coconino Plateau is likely another important source of recharge. The Coconino aquifer is fully saturated in the far eastern and southeastern portions of the study area but mainly occurs as relatively small and discontinuous perched water-bearing zones across most of the study area (Bills et al. 2007). Perched groundwater can be in direct contact with mineralized breccia pipes where they intersect the Coconino aquifer (Alpine 2010). Depth to water ranges from 10s of meters to more than 300 m below land surface (US Geological Survey 2019a). Groundwater in the Coconino aquifer generally flows to the north and discharges at South Rim springs, which are usually smaller in discharge volume than Redwall-Muav aquifer springs, or percolates deeper into the subsurface via faults and fractures through 300 m or more of unsaturated Supai Group (Hart et al. 2002; Monroe et al. 2005; Bills et al. 2007).

The Redwall-Muav aquifer consists of the limestone and sandy limestone members of the Redwall, Temple Butte, and Muav Limestones which are stratigraphically confined by fine-grained sediments of the overlying lower Supai Group and the underlying Bright Angel Shale (Fig. 2). Most Redwall-Muav aquifer springs discharge along or near the lower contact with the Bright Angel Shale. The Redwall-Muav aquifer is likely recharged by mountain block recharge (a term coined by Manning and Solomon 2003) process near the San Francisco Peaks and downward migration of groundwater from overlying aquifers along fractures, faults, and collapse features (Huntoon 1977; Hart et al. 2002; Bills et al. 2007). A rudimentary potentiometric surface map for the Redwall-Muav aquifer was created from a small number of water levels (Bills et al. 2007) and shows groundwater flow toward large springs in the Little Colorado River (Blue Spring) and Cataract Canyon (Havasu Spring). Groundwater flow is hypothesized to be controlled by five main features: (1) karst systems developed on joint fractures and faults, (2) large regional faults, (3) lithology and regional dip of the rock matrix, (4) incision of the Colorado River and its tributaries through rock units of the aquifer, and (5) the relatively impermeable Bright Angel Shale (Cooley 1976; Huntoon 2000; Bills et al. 2007). The Redwall-Muav aquifer is the primary groundwater flow system discharging to more than 200 known springs in GRCA, several dozen springs on the Havasupai Reservation, and as base flow to short perennial reaches of multiple tributary streams to the Colorado River in the study area.

Data collection and methods

As the primary groundwater aquifer, springs issuing at the contact between Redwall-Muav aquifer hydrogeologic units and the Bright Angel Shale were targeted for sampling. Springs between the Little Colorado River and National Canyon were assessed for hydrologic and geologic characteristics as well as anthropogenic and ecological importance—for example, Havasu Spring is vital for the Havasupai Tribe and is the important water source for the endangered Humpback Chub habitat at the mouth of Havasu Creek (Cataract Canyon). Many springs emerging from the South Rim are at least 900 m below the canyon rim. The springs are usually located at tributary headwaters and can be far from established trails. Sites were accessed by 1–4 day backpack trips or multi-day river trips on the Colorado River limiting samples collected for this study to a small subset of the recognized springs. Sample locations were further constrained by sample collection considerations. The primary concern for

sampling was dissolved noble gases which are very sensitive to contact with the atmosphere or degassing prior to collection. For this study, extensive discussion with previous investigators and reconnaissance was conducted to target sample locations that might be suitable. Sample collection was done as close as possible to the first emergence of water or the main discharge point. Often these points are not colocated, in which case the hydrologist's best-judgment was used for collection of a representative sample.

Twelve springs and 2 wells were sampled between June 2016 and May 2018 for dissolved noble gases (helium, He; neon, Ne; argon, Ar; krypton, Kr; xenon, Xe), stable isotopes of water (delta hydrogen-2, δ^2H; delta oxygen-18, δ^{18}O), tritium (^{3}H), and carbon isotopes (delta carbon-13, δ^{13}C; carbon-14, ^{14}C). Samples for the man-made tracers of chlorofluorocarbons (CFC-11, CFC-12, CFC-113) and sulphur hexafluoride (SF_6) were collected but comparison to ^{3}H, which is considered more reliable, showed the tracers to be contaminated and of limited utility as an age tracer. Field parameters, including water temperature, pH, specific conductance, dissolved oxygen, total dissolved gas pressure, barometric pressure, and discharge were collected at wells and springs immediately prior to collecting the water sample. Alkalinity titrations were performed in the field with the exception of samples from Blue Spring and from 140 Mile and National Canyon Springs which were performed in the laboratory due to site access issues or instrument error in the field. Sample collection and processing and field parameter collection was conducted following USGS protocols (Gibs et al. 2012; Radtke et al. 2002; Ritz and Collins 2008; Rounds and Wilde 2012; Rounds et al. 2013; Skrobialowski 2016; US Geological Survey 2006, 2019b; Wilde et al. 2014; Wilde 2002, 2004, 2006). Due to the remoteness and hazards of accessing sampling sites, exceptions to the standard sample collection and processing, such as pumping rates and refrigeration of samples, were made depending on accessibility and characteristics of each site. Additional detail on sample collection, analytical methods, and tracer systematics are available in the electronic supplemental material (ESM1). Complete field parameters and data are available through National Water Information System (NWIS; US Geological Survey 2019a) and USGS ScienceBase data release (Solder 2020).

Additional groundwater environmental tracer data (^{3}H and ^{14}C) were compiled from previous studies (Monroe et al. 2005; Bills et al. 2007) and from NWIS (US Geological Survey 2019a) providing data for additional sites and time-series data. Supporting field parameters (water temperature, pH, alkalinity) and δ^{13}C were used to correct measured ^{14}C using the methods described in this report for consistency, rather than making use of corrected ^{14}C as reported in the respective publications. If supporting data were not available to facilitate geochemical correction, the ^{14}C value was excluded.

Stable isotope mixing model

The relative contribution to recharge from seasonal precipitation end-members, winter versus summer, was assessed using a δ^2H and δ^{18}O mixing model. Modeled precipitation data for the study area and surface water data were used to define the respective seasonal end-members. Seasonal mixing model results are expressed as the fraction of winter recharge (F_{win}) captured in a given sample. Although elevational influence on δ^2H and δ^{18}O fractionation cannot be ruled out, observational data showed no statistically significant relationship between δ^2H or δ^{18}O in precipitation and elevation across the study area, and thus was not considered in the mixing model. Complete discussion of model construction and evaluation is provided by Solder and Beisner (2020). The values of F_{win} were used in this study to guide conceptual models and provide context to age tracer data.

Noble gas solubility modeling

Dissolved noble gas concentrations of Ne, Ar, Kr, and Xe were interpreted using the closed-equilibrium (CE) model (Aeschbach-Hertig et al. 2000) to determine noble gas recharge temperature (NGT), a proxy for elevation and seasonal timing of recharge, excess air (EA; dissolved dry air at time of recharge), and the fractionation factor (F) of the gases during recharge. Inverse CE models were optimized by minimizing the sum of chi-squared statistic (χ^2) between measured and modeled gas concentrations using the routine of Jung and Aeschbach (2018). A groundwater temperature lapse window, bounded by the observed mean annual air temperature lapse rate and a +3 °C correction to the observed air lapse rate approximating temperature at the water table, was used to constrain maximum and minimum estimates of NGT and recharge elevation following Manning and Solomon (2003). The lapse window approach results in two CE model solutions (two values of NGT and recharge elevation) defining the upper and lower bounds of reasonable recharge conditions as defined by the lapse rates. Additional details of the approach are provided in the ESM1. An important consideration in modeling the noble gas concentrations is the addition of deeply sourced CO_2 (see Crossey et al. 2006) resulting in exsolution of super saturated gas as hydrostatic pressure is reduced. The CE model can capture this condition of degassing with values of F >1 (Aeschbaach-Hertig et al. 2008), but in this study modeled recharge conditions are likely not representative of actual recharge for such samples. Additional discussion of degassed samples is provided later in this report.

Helium source

Stable isotopes of helium (^{3}He and ^{4}He) and neon (^{20}Ne) dissolved in groundwater were used to track fluid and gas

origins. The measured ratio of ^{3}He to ^{4}He (R) are reported relative to the ratio in the atmosphere (R_a; 1.384 x 10^{-6}). By this convention air equilibrated water (AEW) has an R/R_a value of 1 and deviations indicate additional helium sources. Similarly, deviations of the measured ratio of ^{4}He to ^{20}Ne from the atmospheric value (~0.288) is suggestive of nonatmospheric helium source (Ballentine et al. 1991). A helium mass balance was calculated to determine the individual contributions of helium from AEW, EA, and radiogenic sources (i.e., crust, mantle, and decay of ^{3}H [$^{3}He_{trit}$]; Solomon and Cook 2000; Solomon 2000). As no ^{4}He is produced in ^{3}H decay, concentrations of ^{4}He in excess of atmospheric sources (AEW plus EA) can be attributed to terrigenic sources (i.e., crust and mantle). For samples with terrigenic He (He_{terr}) greater than 1×10^{-8} ccSTP/g, $^{3}He_{trit}$ was considered a negligible component of the total helium budget. For samples with minimal He contributions from the atmosphere and ^{3}H-decay, the measured R/R_a was used directly to resolve the fraction of He from crustal and mantle sources. The fraction of mantle helium (F_{SCLM}) was calculated by a binary mixing model assuming a crustal R/R_a value ranging from 0.15 to 0.02, representative of deep bedrock sources (Mamyrin and Tolstikhin 1984; Stute et al. 1992; Castro et al. 1998) and uranium- and thorium-series decay (Andrews 1985), respectively, and an R/R_a value of 6 for subcontinental lithospheric mantle (SCLM), likely representative of mantle sources in the study area (Gautheron and Moreira 2002).

Carbon-14 geochemical correction

Analytical correction methods (Revised Fontes and Garnier model; Han and Plummer 2013) were used to correct ^{14}C prior to estimating groundwater age. Graphical methods (Han et al. 2012) were used to better constrain the isotopic end-members and interpret the correction models. Soil CO_2 was expected to have ^{14}C of 100 percent modern carbon (pmc) and $\delta^{13}C$ of –21 ‰ in part based on reported soil gas compositions in the mountainous southwest (Huth et al. 2019). Aquifer carbonate was expected to have ^{14}C of 0 pmc and $\delta^{13}C$ ranging from 2 to –5 ‰ based on measured values of $\delta^{13}C$ in carbonate rocks (Muller and Mayo 1986; Saltzman 2002; Bills et al. 2007). A final $\delta^{13}C$ value of 2 ‰ was selected based on graphical guidance (Han et al. 2012), reasonability of modeled results, and previous investigations of South Rim carbon isotopes (Crossey et al. 2006). Final adjusted ^{14}C was used for age interpretations.

Groundwater age

Recognizing that a groundwater sample is a mixture of flow paths with varying ages, groundwater age was characterized in this study by lumped parameter model (LPM) estimated mean age and age distribution. The age distribution represents the probability of a water parcel with a given estimated age occurring in the sample. A modified version of TracerLPM (Jurgens et al. 2012; B. Jurgens, US Geological Survey, personal communication, 2019) was used to evaluate temporal tracer stability and fit LPMs to individual samples. Published historical atmospheric concentration time-series for ^{3}H and ^{14}C (Michel et al. 2018 and Reimer et al. 2013, respectively) were input to TracerLPM. Age distribution parameters (i.e., LPMs) for individual samples were varied to minimize the misfit, quantified as the χ^2 between measured and simulated concentrations of the select modeled tracers.

Additional discussion of noble gas solubility modeling, helium source systematics and interpretation, complete ^{14}C geochemical model input, description of LPM models and criteria for selection, and groundwater age interpretations are available in the ESM1.

Results

Noble gas solubility modeling

The CE model estimated recharge conditions explain the measured noble gas concentrations with χ^2 values less than the critical value (3.84; one-sided, one degree of freedom, 95% confidence) for all samples (Table 1), except for Fern Spring at an estimated recharge elevation of 2080 m ($\chi^2 = 5.07$). For CE models with a defined value of $F < 1$ (140 Mile, Horn Creek, Indian Garden, National Canyon, and Pipe Creek Springs), the modeled results are representative of recharge conditions and modeled NGT ranges from 3.7 to 20 °C and EA ranges from 5×10^{-4} to 0.12 ccSTP/g. Terrigenic He is generally small in these samples, indicative of a large component of atmospheric He, which is reflected in R/R_a values near 1 (Table 1). The remaining models with F greater than 1 are degassed and, as discussed later, modeled recharge conditions for these sites are less certain. Modeled He_{terr} for sites with F greater than 1 is very high and accounts for more than 90% of the total He (He_{tot}) in the samples.

Environmental tracers and groundwater age

The full data set, including newly collected samples and samples compiled from literature, contained groundwater age tracer data (^{3}H and/or ^{14}C) from 33 sites, with multiple observations available at 19 sites (Table 2). Samples for tracer data were collected between August 1994 and May 2018 in roughly three separate periods in the mid-1990s, early-2000s, and throughout the 2010s for the various investigations. For sites sampled multiple times the average period of record is approximately 13 years. In total, the full data set had 63 ^{3}H samples with most samples ($n = 55$) having detectable ^{3}H (Table S1 of the ESM2). The full data set had a total of 51 ^{14}C samples,

Table 1 Noble gas solubility modeling results and select isotopes. USGS station ID, latitude, longitude, and elevation of sample locations are provided in Table S1 in the ESM2. Recharge elevation relative to North American Vertical Datum (NAVD88). χ^2 chi-square of model fit, χ^2 *Prob.* probability of model fit, *EA* excess air, *F* fractionation factor, *NGT* noble gas recharge temperature, *ccSTP/g* cubic centimeters per gram at standard temperature (25° C) and pressure (1 atm), *R* sample ratio of helium-3 to helium-4, R_a ratio of helium-3 to helium-4 in air, F_{SCLM} fraction of helium from subcontinental lithospheric mantle (*SCLM*) sources

Map ID	Site name	Recharge Elev. (m)	χ2	χ2 Prob. (%)	EA (ccSTP/g)	*F*	NGT (°C)	Fitted gases	He_{terr} (ccSTP/g)	He_{terr}/ He_{tot}	$^3He_{trit}$ (ccSTP/g)	R/R_a	$^4He/^{20}Ne$	F_{SCLM}
1	140 Mile Spring	1,650	1.44	23.1	0.097	0.80	15.2	Ne, Ar, Kr, Xe	6.49E-09	0.124	1.36E-15	0.882	0.300	–
		1,220	1.83	17.6	0.105	0.84	16.1	Ne, Ar, Kr, Xe	6.28E-09	0.120	1.13E-15			
24	Horn Creek Spring	2,930	0.59	44.2	6.7E-03	0.74	3.7	Ne, Ar, Kr, Xe	2.91E-09	0.069	2.71E-15	0.963	0.268	–
		2,430	0.42	51.8	1.4E-03	0.58	5.2	Ne, Ar, Kr, Xe	2.49E-09	0.059	2.19E-15			
25	Indian Garden Spring	1,920	0.002	96.2	9.2E-03	0.90	12.8	Ne, Ar, Kr, Xe	2.68E-09	0.065	5.11E-16	0.928	0.275	–
		1,380	0.06	81.1	5.3E-05	~0	14.7	Ne, Ar, Kr, Xe	2.50E-09	0.061	3.27E-16			
32	National Canyon Spring	1,415	1.22	26.9	0.112	0.85	17.3	Ne, Ar, Kr, Xe	4.08E-09	0.085	4.10E-15	0.962	0.291	–
		1,000	1.60	20.6	0.119	0.90	18.1	Ne, Ar, Kr, Xe	3.91E-09	0.081	3.91E-15			
35	Pipe Creek Spring	2,765	0.04	83.4	2.2E-03	0.53	5.2	Ne, Ar, Kr, Xe	2.56E-09	0.058	2.52E-15	0.969	0.271	–
		2,240	0.05	82.2	1.2E-03	~0	6.9	Ne, Ar, Kr, Xe	2.26E-09	0.051	2.17E-15			
4	Blue Spring	1,160	1.28	25.7	ND	1.26	19.7	Ne, Ar, Kr, Xe	1.16E-05	0.997	–	0.668	98.5	0.09–0.11
		960[a]	1.13	28.8	ND	1.29	20.0	Ne, Ar, Kr, Xe	1.16E-05	0.997	–			
8	Canyon Mine observation well	1,930	7.27E-23	–	3.5E-04	–	12.7	Ne, Ar	2.36E-06	0.984	–	0.161	16.3	0–0.02
		1,680[a]	1.81E-23	–	1.7E-04	–	13.9	Ne, Ar	2.36E-06	0.984	–			
14	Fern Spring	2,080	5.07	2.4	6.2E-02	0.96	11.3	Ne, Ar, Kr, Xe	4.12E-06	0.991	–	0.161	28.8	0–0.02
		1,630	1.39	–	ND	1.02	12.4	Ne, Kr, Xe	4.12E-06	0.991	–			
19	Grapevine Main Spring	1,800	3.80	–	ND	1.43	13.9	Ne, Kr, Xe	1.66E-09	0.043	2.29E-15	0.982	0.277	–
		1,420[a]	6.84E-24	–	–5.7E-04	0.95	15.6	Ne, Kr, Xe	3.01E-10	0.008	4.77E-16			
20	Havasu Spring	1,540	1.64	–	ND	1.15	16.2	Ne, Kr, Xe	1.14E-05	0.997	–	0.153	91.4	0–0.02
		1,130	1.42	–	ND	1.21	16.9	Ne, Kr, Xe	1.14E-05	0.997	–			
21	Havasupai well	1,450	1.45	22.9	ND	1.45	17.0	Ne, Ar, Kr, Xe	1.06E-05	0.997	–	0.152	97.9	0–0.02
		970[a]	1.55	21.3	ND	1.55	18.5	Ne, Ar, Kr, Xe	1.06E-05	0.997	–			
23	Hermit Spring	1,445	0.13	71.7	ND	1.10	17.1	Ne, Ar, Kr, Xe	4.14E-07	0.922	–	0.088	3.3	0–0.01
		1,200[a]	0.15	69.8	ND	1.14	17.9	Ne, Ar, Kr, Xe	4.14E-07	0.921	–			

[a] Lower recharge elevation defined by site elevation

ND Excess air not defined for degassed (i.e., $F > 1$) samples

Table 2 Summary of environmental tracer concentrations and groundwater-age lumped-parameter model results. USGS station ID, latitude, longitude, and altitude of sample locations provided Table S1 in the ESM1. Values used to calculate the average (Avg.) and standard deviation (s.d.) are provided in Table S1 in the ESM1. TU = tritium units, pmC = percent modern carbon. Mixing model used to calculate fraction of winter recharge (F_{win}) described by Solder and Beisner, 2020.

Map ID	Site Name	Aquifer	Start Date	End Date	Period of Record (years)	Avg. ^{3}H (TU)	^{3}H s.d.	Avg. ^{14}C (pmC)	^{14}C s.d.	Avg. Mean Age (years)	Mean Age s.d.	Avg. F_{win}	F_{win} s.d.
1	140 Mile Spring	Redwall-Muav	2/23/2018	2/23/2018	—	2.30	—	101.4	—	175	—	0.87	0.13
3	Bar Four Well	Redwall-Muav	5/1/2002	5/1/2002	—	—	—	14.9	—	19100	283	1.25	0.23
4	Blue Spring	Redwall-Muav	6/29/2001	5/15/2018	16.9	0.1	0.08	22.6	6.7	14833	3414	0.93	0.11
5	Boucher East Spring	Redwall-Muav	4/8/2017	4/8/2017	—	0.6	—	49.95	—	9700	141	0.93	0.11
6	Boucher Spring	Redwall-Muav	4/25/2002	4/25/2002	—	2.69	—	—	—	370	—	0.92	0.14
7	Burro Spring	Redwall-Muav	4/29/1995	10/24/2012	17.5	1.14	0.53	58.9	63.7	1000	163	1.02	0.12
8	Canyon Mine Observation Well	Coconino	7/20/2017	1/31/2018	0.5	0.03	0.05	32.8	1.1	10644	532	0.88	0.09
9	Canyon Mine Well	Redwall-Muav	5/20/2003	9/14/2017	14.3	0.08	0.12	29.4	1.4	12040	674	1	0.08
14	Fern Spring	Redwall-Muav	8/24/1994	10/12/2016	22.1	0.21	0.15	75.8	22.6	4485	5254	0.95	0.14
18	Grapevine East Spring	Redwall-Muav	11/12/1994	11/14/2001	7	0.7	0.56	—	—	1976	960	0.68	0.08
19	Grapevine Main Spring	Redwall-Muav	4/30/2001	5/19/2018	17.05	0.48	0.02	102.7	4.3	345	94	1.08	0.10
20	Havasu Spring	Redwall-Muav	8/23/1994	10/11/2016	22.1	0.16	0.22	27.3	1.2	16550	212	0.96	0.14
21	Havasupai Well	Redwall-Muav	8/23/1994	10/12/2016	22.1	0.31	0.44	31.5	14.6	15500	3960	0.95	0.14
22	Hawaii Spring	Redwall-Muav	5/25/2000	4/11/2001	0.9	0.4	0.12	37.7	43.6	4400	115	0.97	0.08
23	Hermit Spring	Redwall-Muav	11/19/2001	4/9/2017	15.4	0.3	0.35	60.6	7.9	6150	3176	0.97	0.07
24	Horn Creek Spring	Redwall-Muav	5/22/2000	5/1/2018	17.9	1.8	0.79	70.3	65.2	356	125	0.97	0.07
25	Indian Garden Spring	Redwall-Muav	10/23/2012	9/27/2016	3.9	—	—	71.5	2.2	2750	289	1.03	0.07
26	JT Spring	Redwall-Muav	4/8/2001	10/24/2012	11.5	0.85	0.36	105.9	3.8	980	28	0.86	0.13
27	Lonetree Spring	Redwall-Muav	4/11/2001	4/11/2001	—	1.5	—	132.8	—	710	—	0.98	0.14
28	Matkatamiba Spring	Redwall-Muav	1/21/2002	1/21/2002	—	0.69	—	73.7	—	1200	—	0.95	0.09
29	Miners Spring	Redwall-Muav	5/24/2000	10/23/2012	12.4	0.63	0.22	—	—	1433	115	1	0.10
30	Mohawk Canyon Spring	Redwall-Muav	9/18/2001	9/18/2001	—	0.09	—	108	—	107	18	0.9	0.14
31	Monument Spring	Redwall-Muav	12/5/2000	11/19/2001	0.96	0.47	0.10	52	40.3	2930	1508	0.986	0.07
32	National Canyon Spring	Redwall-Muav	1/6/1995	2/27/2018	23.1	2.16	1.47	51.3	59.2	87	28	0.95	0.11
33	NPS Wupatki HQ Well	Coconino	7/9/1996	7/9/1996	—	0.31	—	—	—	79	27	0.80	0.13
34	Patch Karr Well	Redwall-Muav	4/13/2004	4/13/2004	—	0.18	—	27.4	—	13200	707	0.94	0.19
35	Pipe Creek Spring	Redwall-Muav	5/22/2000	9/26/2016	16.3	0.84	0.32	71.4	50.1	1047	426	1.02	0.10
38	Red Canyon Spring	Redwall-Muav	8/23/2001	8/23/2001	—	0.7	—	97	—	1500	—	1.05	0.15
39	Royal Arch Spring	Redwall-Muav	3/23/2002	5/24/2018	16.2	1.14	0.67	88.7	4.1	2383	933	0.92	0.14
41	Salt Creek Spring	Redwall-Muav	5/23/2000	10/24/2012	12.4	0.59	0.35	74.4	65.1	1000	183	0.98	0.08
44	Serpentine Spring	Redwall-Muav	4/21/2002	4/21/2002	—	0.5	—	—	—	2000	141	0.98	0.14
45	SF Peaks Well	Volcanic	7/2/1996	7/2/1996	—	10.31	—	—	—	6	—	1.26	0.13
47	Sunset Crater Well	Supai	8/17/2017	8/17/2017	—	—	—	79.6	—	2000	173	0.96	0.19

including the ancillary $\delta^{13}C$, pH, water temperature, and alkalinity data needed for ^{14}C geochemical adjustment. Final adjusted ^{14}C ranged from about 15 to 130 pmc (Table S2 of the ESM2). Following the graphical method of Han et al. (2012), samples that fall below the ^{14}C versus $\delta^{13}C$ carbonate equilibrium evolution line (the so-called zero age line) are predicted to have some radio-decay (i.e., final adjusted $^{14}C < 100$ pmc) and ^{14}C alone can be used to assign an age ($n = 29$). The remaining samples with final adjusted ^{14}C values greater than 100 pmc are useful for more complex LPMs that account for mixing processes which introduce bomb-pulse ^{14}C. In the full data set, a total of 70 unique sets of tracer concentrations were used to estimate groundwater mean ages (Table S1 of the ESM2). A statistical summary for each site, including the range of sample collection dates, tracer concentrations, LPM mean ages, and F_{win} (from Solder and Beisner 2020), is provided in Table 2.

CFCs and SF_6 samples were collected for this study from 12 and 10 sites, respectively (US Geological Survey 2019a). Data values from duplicate bottles were in good agreement (represented by standard deviation of duplicates), with the exception of SF_6 from Blue, Horn Creek, and Pipe Creek springs, and replicate analysis of CFCs from Indian Garden Spring (data not reported) was within 5% of each other. While contamination during sampling is not entirely ruled out, the high quality of duplicate and replicate sample data suggests elevated concentrations are present in the groundwater. Unfortunately, contamination of CFCs and SF_6 (i.e., above expected atmospheric concentrations when compared to ^{3}H) excludes them from use in age dating and no further analysis was conducted.

Discussion

Stable isotope mixing model

Values of F_{win} are less than 0.9 for a large number of sites, indicating that summer precipitation is a measurable contribution to recharge at those sites (Table 2 and Table S1 of the ESM2). Spatially, lower values of F_{win} occur in springs below the South Rim, in the western regions of the study area, and in springs located in large surface water catchments. The largest values of F_{win} are located near the San Francisco Peaks, the eastern Coconino Plateau, and from Redwall-Muav aquifer wells (Solder and Beisner 2020). These results imply that local groundwater recharge from summer precipitation occurs in select locations, and can be a major contribution to spring discharge, although the regional groundwater flow system is mostly recharged by winter precipitation.

Noble gases

On the South Rim, spring discharge emerges from cracks, karst features, and alluvium such that it is difficult, if possible at all, to collect high quality gas samples. Additionally, high concentrations of CO_2 which begins to exsolve under the reduced hydrostatic pressure at Blue Spring and Cataract Canyon locations (Havasu and Fern springs and Havasupai well) present a challenge in sampling water, as much as is possible, before gas loss. Knowledge of the sample collection and site conditions was used to critically evaluate the solubility model results. Future use of the dissolved gas data in this study should consider these limitations.

For samples where no degassing is indicated ($F < 1$; Table 1), the CE model results provide good indication of recharge conditions and modeled recharge conditions can be reasonably explained by the groundwater temperature lapse rates from the study area (Fig. 3). In other words, noble gas concentrations could be modeled by combinations of recharge elevation and temperature that agree with the observed air temperature lapse rate and estimated (+3 °C) water table temperature lapse rate. Although the San Francisco Peaks are volcanic in origin and relatively young, implying a higher than average geothermal heat flow, borehole temperatures (Sass et al. 1982) indicate the deeper geothermal system is decoupled from shallow groundwater where recharge occurs (Morgan et al. 2004). Of importance for this study, borehole temperatures extrapolated to land surface fall within the estimated lapse rates (Fig. 3) suggesting the +3 °C correction between air and water-table temperature is reasonable and no additional local correction to the lapse rate is needed.

Two groups of samples with $F < 1$ are evident based on EA. Indian Garden, Pipe, and Horn Creek Springs have small EA (< 0.01 ccSTP/g) suggestive of relatively slow changes in water table elevation in porous media, or recharge occurring in fractured media with less likelihood of entrapping air. Pipe and Horn Creek Springs have cool NGTs (3.7 to ~7 °C) which indicate dominant recharge during the cooler months at the high elevations (2,240–2,930 m). Indian Garden has a similar EA but warmer NGTs (~13–15 °C) and lower recharge elevation (1,380–1,920 m) consistent with recharge during the warmer spring and summer months on the Coconino Plateau or local to the spring. 140 Mile and National Canyon springs have high EA (~0.1 ccSTP/g) suggestive of rapid changes in water tables or rapid infiltration of water from the surface capturing large amounts of EA (Heaton and Vogel 1981). Warm NGTs (15.2–18 °C) and low recharge elevation (1,000–1,650 m), in addition to high EA, may indicate recharge from surface runoff discharging at 140 Mile and National Canyon Springs.

The CE model results for degassed samples ($F > 1$) need to be carefully considered and, in the case of the South Rim samples, are likely not representative of recharge conditions.

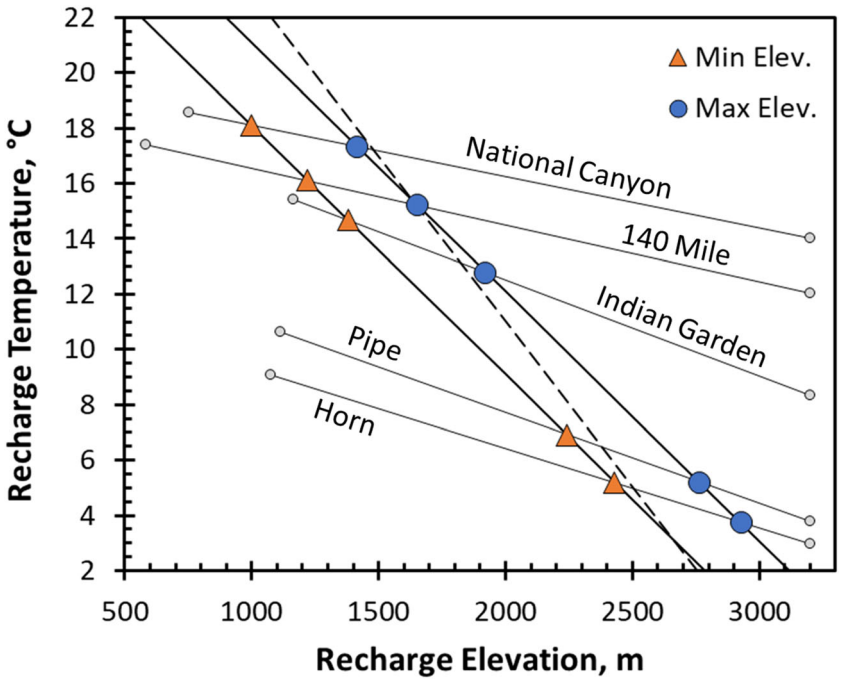

Fig. 3 Plot of noble gas modeled recharge temperature versus recharge elevation for samples with CE modeled values of $F < 1$ (see Table 1). Upper and lower bounds of recharge temperatures indicated by orange triangles and blue circles, with the CE modeled lapse rate (gray lines) for given samples (black text) indicated. Solid black lines indicate the lapse window and the dashed black line indicates the extrapolated geothermal temperature gradient from Sass et al. (1982).

Degassed samples (i.e., $F > 1$), as well as Canyon Mine Observation well, have consistently warm NGTs (11.3–20 °C) and lower recharge elevations (2,080–960 m; Table 2). The other notable feature of degassed samples, except for Havasu and Fern Springs, is the lower estimated recharge elevation as defined by the lapse rate is less than the site elevation (Table 2), indicating modeled NGTs are likely too warm. In these cases, the calculated minimum NGT was based on estimated sample location elevation. Although it is possible that the estimated lapse rate is too shallow, suggesting the mean annual air temperature underpredicts water table temperatures at lower elevations, a more plausible explanation is the ratios of noble gases captured at the time of recharge were subsequently lost due to gas loss and re-equilibration. For Havasu and Fern Springs where the lapse rate does define a reasonable lower recharge elevation, the presence of high dissolved CO_2 concentrations (Crossey et al. 2009) suggest the CE model results are not entirely reliable indicators of the recharge conditions. Also, likely a result of degassing, the CE model could not be fit to the full suite of gases at four sites: Canyon Mine well, Fern, Grapevine Main, and Havasu Springs (Table 2). Comparison to the other model results and inspection of Monte Carlo realizations for the CE model at these sites suggest the presented model solutions are reasonable explanation of the gas concentrations but are likely not representative of actual recharge conditions.

Helium source

South Rim groundwater is separated into two distinct groups based on the ratio of $^4He_{terr}$ relative to $^4He_{tot}$ and by the measured ratio of ^4He to ^{20}Ne (Table 1). Significant He_{terr} (1×10^{-8} ccSTP/g) indicates capture of older water with longer (e.g., crustal He from U- and Th-series decay) and/or deeper (e.g., bedrock or mantle He) flow paths resulting in accumulation of He_{terr}. Values of $^4He/^{20}Ne >> 0.288$ are further indication of large accumulations of He_{terr} in the sample (Ballentine et al. 1991). Samples with lower amounts of He_{terr} and $^4He/^{20}Ne$ approx. equal to 0.288 indicate relatively younger water and atmospherically sourced helium, respectively. A plot of R/R_a versus $^4He/^{20}Ne$ shows the clear separation of the sites based on the contribution of atmospheric sources to the measured ^4He in the sample (Fig. 4). Samples on the left-hand side are dominated by ^4He from AEW while samples on the right-hand side are dominated by nonatmospheric ^4He from terrigenic sources. With the exception of Hermit and Blue Springs, as spring samples accumulate more He_{terr} the R/R_a values converges toward a value of 0.15 (Fig. 4) which is likely a representative end-member of the bedrock radiogenic helium source. For samples with negligible atmospheric ^4He contributions, calculated values of F_{SCLM} suggest a relatively small contribution of mantle sourced He (0–2%, except for Blue Spring with ~9–11%; Table 1). The dominant contribution of crustal He indicates He_{terr} is mostly accumulated during travel along long and deep flow paths in the aquifer, rather than extensive exchanges with deeply sourced mantle fluids.

Fractionation of ^3He relative to ^4He during gas dissolution/exsolution or exchange with an external secondary gas phase will impact measured R of the sample. The simplified case of a single stage of degassing is discussed by Aeschbach-Hertig et al. (2008) where timing of gas loss is critical in determining

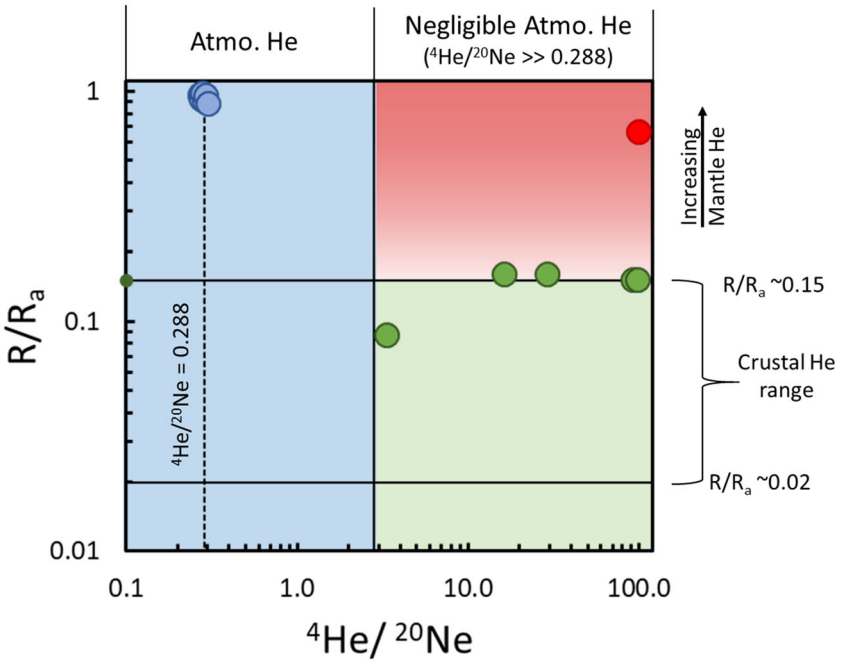

Fig. 4 Plot of R/R_a versus $^4He/^{20}Ne$ with shaded areas indicating He source—atmosphere (blue); crust (green); and mantle (red). Samples indicated by blue circles contain negligible terrigenic He with $^4He/^{20}Ne$ ratios near the atmospheric value of 0.288 (dotted vertical line), green circles and red circles contain negligible atmospheric He, with $^4He/^{20}Ne$ ratios greater than 2.9 (10 times the atmospheric ratio; solid vertical line). Green circles correspond to samples which have no to very little mantle He (F_{SCLM} < ~2%). The red circle indicates Blue Spring which contains between 9 and 11% mantle He (see Table 1)

the impact on helium source component separation. In the case of the South Rim springs, degassing of CO_2 is a late-stage process such that the composite R, with atmospheric and secondary aquifer He, will be affected. Degassing causes preferential loss of ^3He (Bourg and Sposito 2008) and thus a decrease in R and a smaller apparent contribution of mantle He. In the more complicated case of exchange with a secondary gas phase, the He concentration and R in the gas phase relative to the groundwater will determine the effect on R dissolved in the sample. Along the structural and karstic preferential flow paths, the exchange is likely a dynamic process where the secondary exsolved gases and flowing groundwater exchange with multiple gas reservoirs of differing compositions. While it is out of the scope of this study to address the complexity of He isotope fractionation, the authors believe the presented analysis does provide some utility as supporting evidence for differentiating between old groundwater flow pathways. R/R_a values for Havasu Spring are similar to those reported by Crossey et al. (2006; 0.16–0.14, assuming negligible atmospheric He) from free gas bubbles collected in inverted funnels at the same site.

Carbon-14 geochemical correction

Geochemical processes other than radioactive decay act to dilute the atmospheric contribution of ^{14}C required for age dating, resulting in an overestimation of groundwater age (Han and Plummer 2013). Carbon mass and isotope exchange between DIC, soil CO_2, and aquifer carbonate rock are likely to be the primary processes affecting DIC in the South Rim aquifers. Analytical correction methods (Revised Fontes and Garnier model; Han and Plummer 2013) are expected to reasonably account for these processes. Additional geochemical conditions and processes influencing ^{14}C not accounted for in the analytical model are indicated at select sites (Table S2 of the ESM2; Han et al. 2012)—for example, at 140 Mile Spring, the graphical method indicates silicate weathering with the net effect being underprediction of carbonate dissolution and overestimation of mean age. At Horn Creek Spring, CO_2 gas loss is indicated which reduces both $\delta^{13}C$ and ^{14}C of DIC having opposite effects on the adjusted ^{14}C and the net effect of which is difficult to determine without further geochemical modeling.

Water from Blue, Fern, and Havasu springs, as well as Havasupai well had excess CO_2 that is likely derived from geogenic sources (Crossey et al. 2006). Based on the helium source analysis (Table 1), most of the excess CO_2 is likely derived from volcanic sources as opposed to a mantle source. In terms of age dating, correction for the effects of geogenic CO_2 is challenging and, as suggested for this study, cannot be reliably separated from aquifer–rock interactions using $\delta^{13}C$ alone. The relatively close resemblance of geogenic CO_2 (^{14}C = 0 pmc, $\delta^{13}C$ = -5.5‰; Clark and Fritz 1997; Crossey et al. 2006) to carbonate rock (^{14}C = 0 pmc, $\delta^{13}C$ = 2‰) in the region compared to recharge zone sources ($\delta^{13}C$ = 22‰) make separation between the geogenic CO_2 and aquifer sources highly uncertain and no such separation was attempted.

Although this study does not quantitively account for additions of geogenic CO_2, the relative impact on adjusted ^{14}C can be reasonably inferred. According to the model of Han and Plummer (2013), bicarbonate (HCO_3^-) in equilibrium with geogenic CO_2 will have a $\delta^{13}C$ of ~2.8‰, while HCO_3^- in equilibrium with the assumed aquifer rock will have

$\delta^{13}C$ ~1.3‰. Recognizing that measured pH and DIC in the groundwater sample reflect the mixture of the relatively shallow groundwater and geogenic fluids such that carbonate speciation is reflective of the mixture, not accounting for geogenic CO_2 results in an undercorrection of ^{14}C and overestimation of groundwater age at the selected sites. Subsequent calcite precipitation observed at Blue Spring and Cataract Canyon locations was not considered as tufa calcite deposits were not observed directly at the spring orifices where the samples were collected.

The final unaccounted-for process identified that potentially affects adjusted ^{14}C is dedolomitization, that is the process of calcite precipitation and dolomite dissolution driven by addition of Ca from dissolution of gypsum (Plummer et al. 1990). Carbonate (CO_3^{2-}) incorporated into the precipitating calcite has a ^{14}C greater than 0 pmc (mixture of atmospheric and aquifer sources) and CO_3^{2-} from dolomite dissolution has ^{14}C = 0 pmc; the net result of dedolomitization is decreasing ^{14}C of DIC as the reaction progresses. If dedolomitization is unaccounted for, the adjusted ^{14}C is underestimated and the groundwater age is overestimated. Observed concentrations of SO_4^{2-} above 600 mg/L and saturation indices indicative of calcite and dolomite precipitation and dissolution, respectively, observed at Bar Four well and Matkatamiba Spring (Beisner et al. 2020) is suggestive of dedolomitization (Plummer et al. 1990). Additional geochemical modeling required to address the influence of excess CO_2 and dedolomitization on ^{14}C corrections is outside the scope of this study. Based on the aforementioned processes, the reported estimates of ^{14}C based groundwater ages for Blue, 140 Mile, Fern, and Havasu springs, and Havasupai and Bar Four wells should be considered as a probable maximum (Table 2).

Groundwater age

The presence of detectable ^{3}H and relatively low ^{14}C in many springs across the study area (Table 2 and Table S1 of the ESM2) is clear indication the groundwater contains a fraction of modern water recharged since about 1950, and modern water is likely being mixed with older groundwater at many springs. Lumped parameter models (LPMs) were used to model tracer concentrations resulting from mixtures of modern and older groundwater. The conceptual hydrology of the South Rim—developed based on the hydrogeology, stable isotopic mixing models (F_{win}; Solder and Beisner 2020), noble gas solubility model results, helium isotopes, and age tracer concentrations—was used to constrain reasonable selection of LPMs. An iterative process of LPM selection and modeling was adopted as the conceptual model was revised throughout the analysis. Although the conceptual model provides important insights, more complex LPMs that may better represent the physical complexity of recharge sources and the groundwater flow-system are underdetermined; the lack of data for multiple tracers dictated that a conservative approach was taken where simplified LPMs were selected for most sites. Description of the considered LPMs and final LPM results for each sample are provided in ESM1.

Estimated mean ages of South Rim groundwater range from 6 years old in the recharge zone of the San Francisco Peaks to nearly 20,000 years old at Bar Four well and Blue Spring (Table 2; Fig. 5). Along the South Rim between Red Canyon and Boucher springs, groundwater age is correlated to longitude, increasing from east to west (Fig. 6), similar to $\delta^{2}H$ and $\delta^{18}O$ (Monroe et al. 2005; Solder and Beisner 2020), indicating a source of recharge on the eastern portion of the Coconino Plateau. Variability of LPM parameters, representing the relative amount of flow path mixing and based on estimated ranges of physical aquifer dimensions (see ESM1 for discussion), result in an average 7% error in estimated mean age (Table S1 of the ESM2). Mean ages most sensitive to the LPM parameter variability (>20% error) are less than 400 years, indicating relative insensitivity to LPM parameters for age estimates greater than ~1,000 years. Average variation in mean age (~30%) arising from variation in tracer concentrations over time is significantly larger; only 5 of the 20 sites having multiple samples had less than ~10% variation in estimated mean age (Table S2 of the ESM2). Although the estimated mean ages appear relatively insensitive to assumed LPM parameters, the limited number of age tracers is not sufficient to uniquely define the age distributions to a high level of certainty. As such, additional reporting of metrics that can be derived from the full age distribution such as the age quartiles, was not warranted.

The spatial distribution of estimated mean age shows a clear distinction between where the oldest and youngest groundwaters are located (Fig. 5). Mean ages greater than 10,000 years were estimated for deep groundwater from Coconino Plateau wells (including Bar Four well) and at the large natural South Rim discharge locations of Blue Spring and Havasu Spring (Table 2). The old ages, which generally increase with distance from the San Francisco Peaks (Fig. 5), of these sites is suggestive of flow path capture from the regional groundwater flow system in the Redwall-Muav aquifer. Interestingly, mean age at the Canyon Mine Observation well screened in the Coconino aquifer is similar to nearby Redwall-Muav aquifer wells. This finding suggests a hydrologic connection in the area of Canyon Mine or similar recharge sources and groundwater velocities to that hydrologic position in the two systems. In a separate setting, old groundwater from Havasupai well (screened in alluvium) is likely from the same source as Havasu Spring upwelling from Redwall-Muav aquifer bedrock.

The younger estimated mean ages less than 400 years (Grapevine Main, Horn, Boucher, 140 Mile, and Mohawk Canyon Springs) and even less than 100 years (SF Peak well,

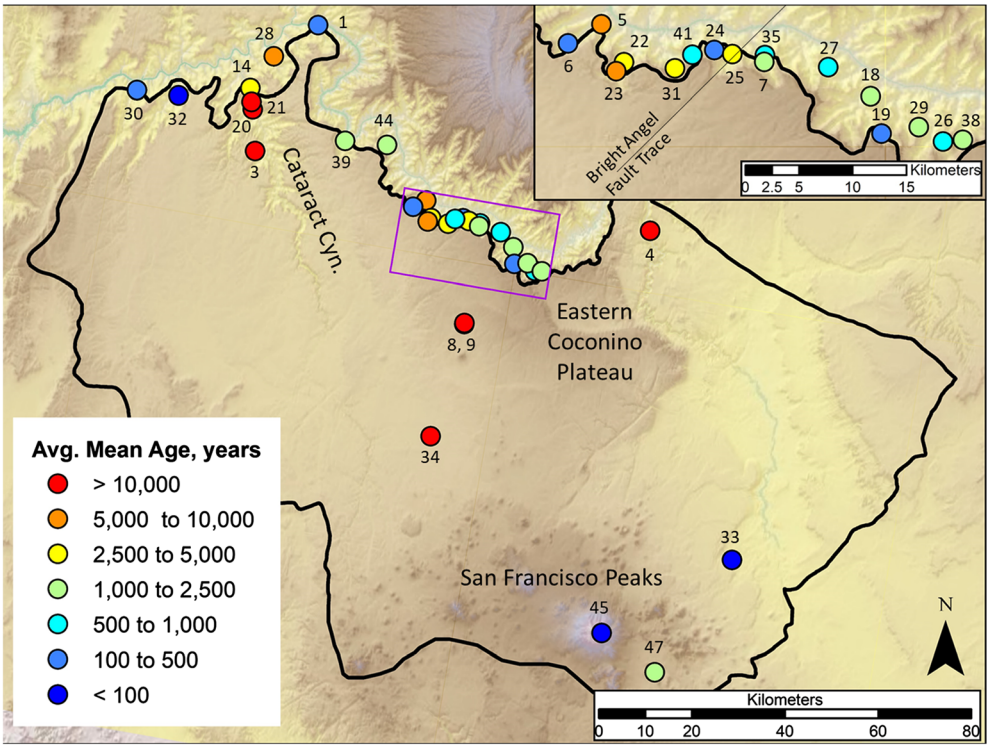

Fig. 5 Map of average estimated mean age. For site names by map ID see Table 2

NPS Wupatki HQ well, and National Canyon Spring) indicate nearby recharge captured at these sites (Fig. 5). SF Peak well is clearly in the snowmelt recharge zone and Waputki HQ well is completed in the unconfined Coconino aquifer where a mixture of SF Peak snowmelt run-off and local precipitation is likely captured. The remaining springs with mean ages between 400 and 10,000 years either contain a single recharge source from an intermediate distance between the San Francisco Peaks and the South Rim, or some mixture of groundwater with varying sources and ages. The statistically significant relationship between age and longitude for springs in the central part of GRCA (Pearson's r = –0.51, p-value = 0.04) with increasing age moving to the west (Figs. 5 and 6) suggests the higher elevation eastern portion of the Coconino Plateau, receiving more annual precipitation, as a potential source of recharge. Unfortunately, the current age tracer data set is not sufficient to confidently define a full age distribution, which is needed to better identify and quantifying the relative contribution of specific recharge sources using age tracers.

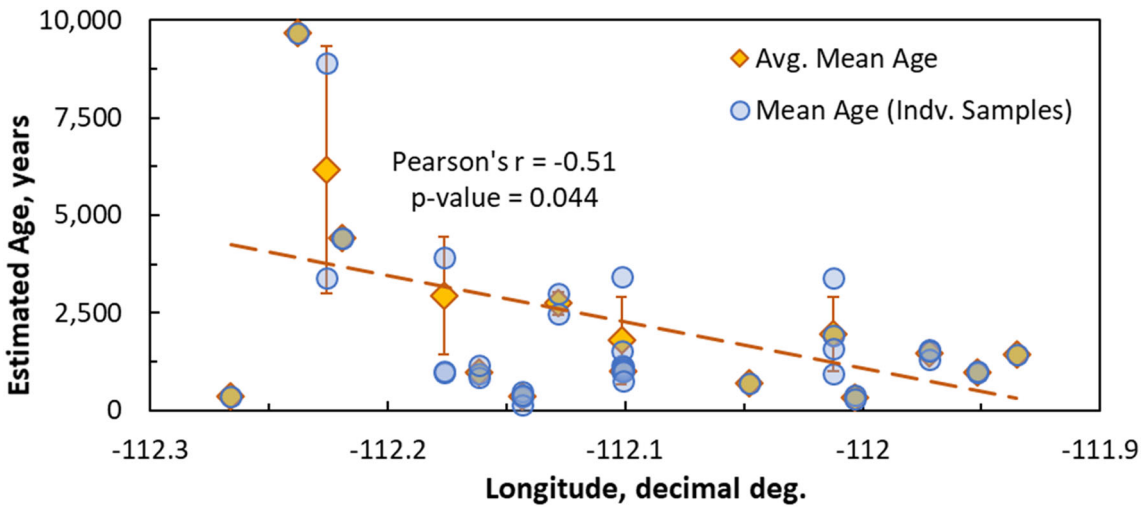

Fig. 6 Estimated mean groundwater age versus longitude for select sites along the South Rim (see inset of Fig. 5). Orange error bars indicate the standard deviation of the mean age, and dashed red line indicates the linear best-fit. Pearson's r correlation coefficient and p-value indicated in black text

Synthesis of results

These results, as well as the results of the companion studies (Solder and Beisner 2020; Beisner et al. 2020), support a new conceptual model for the South Rim groundwater system (Fig. 7). The previous model of distinct physical separation of the Coconino and Redwall-Muav aquifer groundwater flow systems recharged solely from snowmelt off the San Francisco Peaks (Hart et al. 2002; Monroe et al. 2005; Bills et al. 2007) is inconsistent with the tracer data of this study. It is suggested that South Rim groundwater is not only sourced from the regional Redwall-Muav aquifer (as traditionally conceptualized) but also from more-localized sources recharged under a variety of different mechanisms. The synthesized results presented here clearly define two main groundwater sources in an internally consistent conceptual model.

Old water

Deep regional groundwater captured from Redwall-Muav aquifer wells located in the Coconino Plateau and from Blue and Havasu springs is characterized by low ^{14}C (<35 pmc), high $^{4}He_{terr}$ (>1 × 10^{-6} ccSTP/g), and $^{4}He/^{20}Ne$ much greater than the atmospheric value of 0.288 (Tables 1 and 2). Groundwater sampled from Hermit Spring, with an average groundwater age of 6,150 years based on ^{14}C, has an R/R_a value of 0.08, suggesting relatively limited contact with deeper bedrock compared to other old samples that have R/R_a values closer to 0.15 (Table 1; Fig. 4). This suggests that flow paths to Hermit Spring are potentially not as deep as those to other old groundwater springs, maybe a result of the relative lack of major structural features adjacent to Hermit Spring. Estimated F_{SCLM} (0 to ~2%, except Blue Spring ~10%; Table 1; Fig. 4) indicates that He_{terr} is largely accumulated during long transit times rather than exchange with deeper mantle fluids; these findings are consistent with estimated mean ages greater than ~10,000 years. Furthermore, He_{terr} systematically varies (Fig. 8) and has statistically significant correlations with ^{3}H and ^{14}C (Spearman's $\rho = -0.5$ and -0.82, p-value = 0.12 and 0.004, respectively), also suggesting He is accumulated along long flow paths rather than from discrete sources, although mixing of young and old flow paths is evident (i.e., ^{3}H present is samples with high He_{terr}).

Remarkable consistency is found between the average groundwater velocities, calculated as the distance from the San Francisco Peaks to the sample site divided by average estimated mean age, for a karstic system with potential fast-flow conduits. Average groundwater velocity for Sunset Crater, Canyon Mine, Bar Four, Patch Karr wells, Blue, and Havasu springs is 6.5 ± 0.7 m/year and values differ by less than ~20% from the overall mean for these sites, excluding Patch Karr well with a lower velocity. The older groundwater relative to its lateral position at Patch Karr well could be a result of the screened interval position in less permeable portions of the aquifer (i.e., not a solution cavity) but the exact reason is unclear. For comparison, groundwater velocities of North Rim premodern water, calculated assuming a probable maximum lateral distance (between the Kaibab Plateau high point and the spring orifice) and reported mean ages (Beisner et al. 2017b), averaged to be 14.8 ± 8 m/year. The consistency

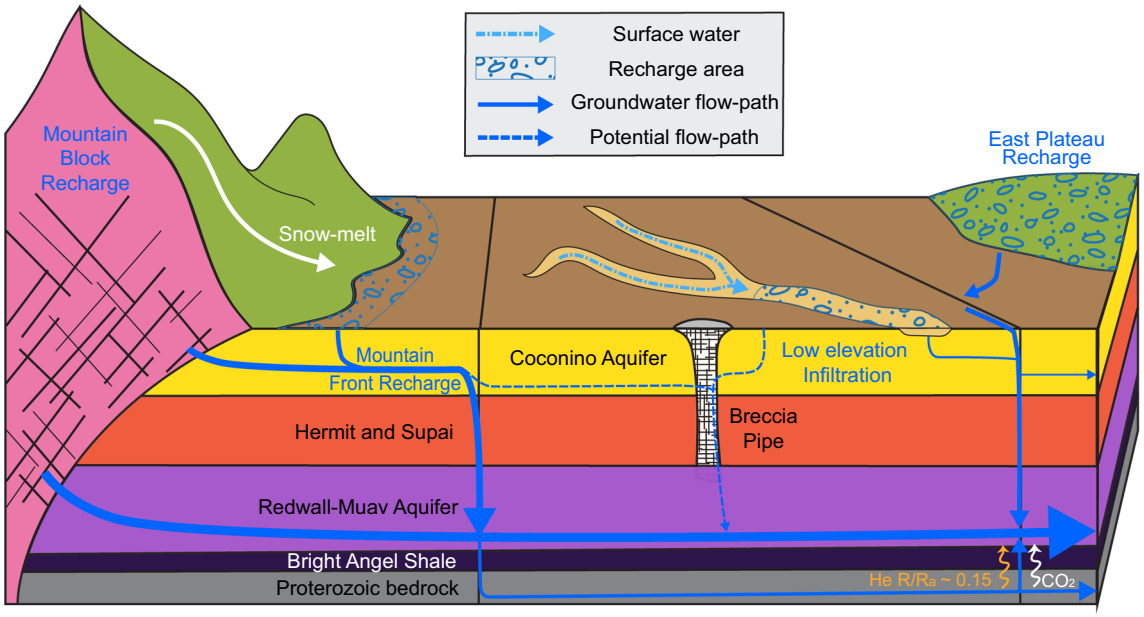

Fig. 7 Conceptual groundwater flow diagram for the South Rim, Grand Canyon, USA. Groundwater recharge sources labeled with blue text. Relative flow amounts indicated by size of flow-path arrows. Hydrogeology generalized from Fig. 2 with major features labeled with black text. Dissolved gases (orange is He; white is CO_2) sourced from bedrock and transported along faults indicated by curvey arrows at bottom right

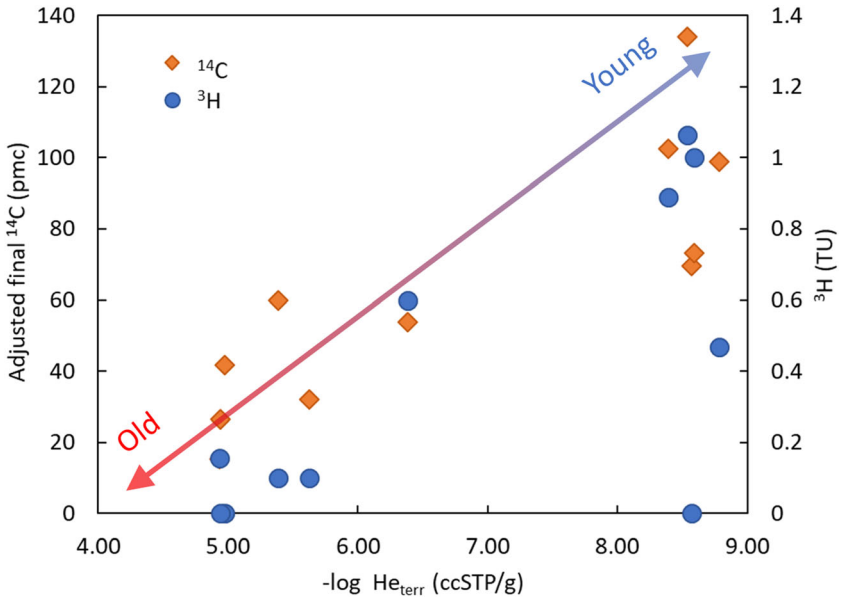

Fig. 8 Plot of terrigenic He (–log He_{terr}) versus ^{3}H and ^{14}C for select sites (see Tables 1 and 2). General trend in tracer concentrations with groundwater age indicated by blue (young) to red (old) arrow

in groundwater velocities, general increase in age moving down hydraulic gradient (Fig. 5), and values of F_{win} greater than ~90% suggest the South Rim deep Redwall-Muav aquifer is primarily recharged from snowmelt on the San Francisco Peaks. This conceptual model for the deep Redwall-Muav aquifer is consistent with previous conclusions of Hart et al. (2002), Monroe et al. (2005), and Bills et al. (2007).

Modern water

Detectable ^{3}H in the majority of groundwater samples (Table 2) and low fractions of He_{terr} in South Rim springs (Table 1; Fig. 8) suggest groundwater distinct from the deep Redwall-Muav aquifer water is captured at many sites. The modern water sources to the South Rim are separated into three groups (see Fig. 7 for conceptual diagram):

Group 1. High elevation snowmelt recharge located within/near the San Francisco Peaks. Group 1 modern water is characterized by high ^{3}H (>5 TU) and F_{win} (~1), for example San Francisco Peaks well, which is the conceptual recharge source for the deep Redwall-Muav aquifer. As discussed later, this modern water source is not observed at South Rim springs.

Group 2. Low elevation surface water infiltration. Group 2 modern water is characterized by modern ^{14}C (>100 pmc) and/or ^{3}H (>1 TU), relatively low F_{win} (<0.9), warm estimated recharge temperatures (>15 °C), and discharging from alluvial sediments in a large surface water basin. Type examples of low elevation surface water infiltration are represented by National Canyon and 140 Mile Springs.

Group 3. Coconino Plateau/South Rim recharge. Group 3 modern water is characterized by moderate ^{3}H (>~0.5 TU), cool recharge temperatures (<7 °C), and high F_{win} (>0.95) as exemplified by Horn Creek, Pipe, and Grapevine Main Springs (with the exception of warm Grapevine NGT which appears to be a result of gas loss).

The proposed surface-water infiltration (group 2) and Coconino Plateau/ South Rim recharge (group 3) modern water sources are distinct from so-called fast-flow pathways, common of karstic systems, although it has similar characteristics to plateau sources. In theory fast-flow could be invoked to reasonably explain the presence of ^{3}H in otherwise old groundwater such Canyon Mine well and Blue and Havasu springs (Table 2) through transport of modern recharge through the regional aquifers from the San Francisco Peaks to the South Rim. Indeed, such a mechanism has been observed on the North Rim of the Grand Canyon where vertical and lateral groundwater velocities as high as 20 and 1 m/day, respectively, were observed using dye-tracing methods (Tobin et al. 2017). While such fast-flow on the South Rim cannot be conclusively ruled out with the current data set, such a mechanism is unlikely based on the conceptual understanding of the flow system and tracer data. Systematic variation of mean age (Fig. 5) and $\delta^{18}O$ (Fig. 7 of Solder and Beisner 2020) in South Rim springs (i.e., decreasing $\delta^{18}O$ values and increasing mean age from east to west; Pearson's r = –0.51 and –0.66, respectively, with 95% confidence) is inconsistent with a heterogeneous fast-flow mechanism along carbonate solution features controlled by faults and fractures. Although mean age is an imperfect measure of fast-flow—the young component of a well-constrained age distribution would be better—the relative similarity of South Rim Redwall-Muav aquifer

groundwater velocities (6.5 ± 0.7 m/year) as compared to the greater variability of North Rim premodern water (14.8 ± 8 m/year) indicate greater spatial homogeneity of South Rim transport mechanisms. As a final point in regard to fast-flow, values of $F_{win} < 1$, particularly at Canyon Mine Observation well screened in the Coconino aquifer ($F_{win} < 0.9$), are more consistent with Coconino Plateau recharge than a fast-flow recharge source that would be largely snowmelt.

Although identifying the presence of young localized groundwater using spring chemistry is fairly straight forward, identifying one of the discussed mechanisms—surface-water infiltration and Coconino Plateau/South Rim recharge—as the most likely source (if possible) requires interpretation of tracer data in context of the hydrogeology, hydrologic position, and surrounding spring chemistry. Given the uncertainty and highly subjective nature of such an interpretation, this study refrains from doing so for all the springs and wells studied in the report.

Controls on groundwater age

The chemistry of the remaining springs not well described by either the deep Redwall-Muav aquifer (e.g., high He_{terr} and mean ages of greater than 10,000 years) or young more local recharge (e.g., some combination of ^{3}H greater than ~0.5 TU, $F_{win} < 1$, and/or cool recharge temperatures) are reasonably explained as a mixture of the two groundwater source end-members. Whereas it has been previously indicated that that structural geologic features (i.e., faults and fractures) are a primary control on groundwater flow paths and spring locations (Huntoon 1977, 2000; Brown and Moran 1979), the tracer data set investigated in this study empirically indicates a hydrogeologic control on spring chemistry as well. Springs located near the Bright Angel and Cataract faults provide good examples of the influence of geologic structure on spring chemistry. Indian Garden Spring is located along the Bright Angel fault and has an older estimated mean age, lower R/R_a, and higher F_{win} (Fig. 5; Tables 1 and 2) than the immediately adjacent Pipe and Horn springs. These trends indicate Indian Garden Spring has a larger fraction of Redwall-Muav aquifer water. Cooler estimated recharge temperatures at Pipe and Horn Creek springs (Table 1) suggest a different recharge source is captured at Indian Garden Spring, although the difference in sources is unclear. Additionally, $^{86}Sr/^{87}Sr$ data reported by Monroe et al. (2005) showed increasingly radiogenic values in springs when approaching the Bright Angel fault. More radiogenic $^{86}Sr/^{87}Sr$ ratios are consistent with capture of groundwater with longer groundwater transit time and more influenced by water–rock interaction with deeper bedrock materials.

As another example, Bar Four, Havasupai wells and Havasu, Fern springs are located near/along the Cataract and Havasu Spring faults. Fern Spring has less nonatmospheric He (lower $^{4}He/^{20}Ne$; Table 1) and a younger mean age (Table 2) than Havasu Spring and Havasupai well suggesting the latter are intercepting groundwater from long deep flow paths. One possible explanation is that Havasu Spring and Havasupai well are located along the Havasu Spring Fault which acts as a preferential flow path of deep Redwall-Muav aquifer groundwater. Interestingly, Bar Four well is located off the Cataract Fault and captures the oldest groundwater, based on an LPM fitted to ^{14}C, with the largest value of F_{win} of the subgroup (Table 2). The difference in Redwall-Muav aquifer water away from the fault (i.e., Bar Four well) versus Havasu and Fern springs, and Havasupai well along the Cataract fault indicate mixing with a small component of an additional groundwater source (i.e., low elevation surface water and/or plateau recharge). Regarding potential capture of plateau recharge, the tracer data could be interpreted to suggest that faults act both as a preferential flow path for Redwall-Muav aquifer water and as a sink for groundwater recharge from the Coconino Plateau. A more probable explanation for the apparent contribution of young groundwater to Havasu and Fern springs, and Havasupai well is run-off infiltration given the large catchment area of Cataract Canyon. Regardless of groundwater sources, the examples from Bright Angel, Cataract, and Havasu Spring faults indicate structural features have a strong influence on the movement and chemistry of South Rim groundwater.

Variability of mean age

The variability in mean ages, expressed as the standard deviation, for a given site (Table 2) apparently contradicts the observed seasonal and long-term relative stability observed in stable isotopes for most sites (Solder and Beisner 2020), but the two findings are not necessarily incongruent. Temporal variability of travel times in the groundwater flow system is driven by recent shifts in climate (2000s drought; MacDonald et al. 2008) and variability in recharge source (snowmelt versus monsoon rainfall/runoff) and recharge location (San Francisco Peaks versus plateau) is on a seasonal and interannual basis. Furthermore, groundwater chemistry and discharge rates of springs do not react instantaneously to changes in recharge rates or chemistry. Lag times in groundwater are the (1) hydraulic lag that is the response time of spring discharge/water-table elevation to changes in recharge rate (i.e., pressure wave), and (2) advective lag that is the elapsed time for a molecule to travel along the flow path (i.e., groundwater age). It is the combination of the hydraulic and advective lags and flow path activation (e.g., Pangle et al. 2017; Kaandorp et al. 2018) that dictate groundwater tracer chemistry in response to variable recharge source and flow paths. With the understanding that groundwater is a mixture of flow paths of varying ages and recharge sources, the lack of variability in stable isotopes measured at the springs (Solder and Beisner 2020) suggests that the long-term isotopic composition of the recharge source is steady. In other words, on a decadal to centurial scale recharge from differing sources is at a quasi-steady state and the mixed stable isotope composition of the groundwater at a given

site is relatively constant. The age tracers differ in that the input concentrations have varied over time and the tracers ^{3}H and ^{14}C radioactively decay. These systematics of ^{3}H and ^{14}C increase the sensitivity to temporal variations of climate, recharge source and location, and lag times as compared to stable isotopes. Unfortuenately, seasonal and long-term variations cannot be clearly distinguished with the current data set. There is some preliminary evidence of short-term (monthly time scale) variations in trace element chemistry and tritium at a perched groundwater spring north of Grand Canyon that warrant further investigation (Beisner and Tillman 2018). Thorough investigation of temporal variability requires more specific sampling design and consideration of the temporal variability in seasonal and interannual hydrologic drivers (i.e., precipitation amount, type, and location, surface-water run-off events, water use), which is outside the scope of this work.

Conclusions

Conservation of groundwater springs as an ecologically, culturally, and economically important resource is in apparent conflict with expanding human activities south of the Grand Canyon which depend on groundwater. Residential expansion and continued extraction of economically valuable mineral resources from the region has raised concerns about potential depletion and contamination of South Rim groundwater. In this study, a suite of environmental tracers was collected, compiled, and analyzed to refine the conceptual model of groundwater recharge sources and flow paths captured at South Rim springs. Such work is important to better understand the potential for changes in discharge and chemistry resulting from alterations to the groundwater flow system. Tracer data collected and compiled included dissolved noble gas concentrations and isotopic ratios, and age tracer concentrations of tritium (^{3}H) and carbon-14 (^{14}C). The main finding was that groundwater captured at South Rim springs originates from two general sources and groundwater tracer chemistry is reasonably explained by the relative contribution of each.

Established conceptual models suggested that the deep Redwall-Muav aquifer is the dominant regional system and primary source to most groundwater discharge locations along South Rim of the Grand Canyon (e.g., Hart et al. 2002; Monroe et al. 2005; Bills et al. 2007). This conceptual model was developed based on the high expected recharge rates on the San Francisco Peaks, regional hydrogeology with physical confinement between the shallow Coconino aquifer and deeper Redwall-Muav aquifer, and the observation that South Rim springs discharge from the Redwall-Muav aquifer,. Findings of Solder and Beisner et al. (2020), that show similarity between $\delta^{2}H$ and $\delta^{18}O$ of groundwater and winter precipitation, and from this study support the idea that the primary source of groundwater to most springs is a deep regional source. The regional groundwater is characterized by high terrigenic-He (> $1x10^{-8}$ ccSTP/g) and estimated mean ages greater than 10,000 years, indicative of long flow paths and travel times, and generally a high fraction of recharge from winter precipitation. Noble gas isotopes indicate that dissolved gases largely originated from atmospheric and crustal sources, including young volcanic rocks, and the limited detection of mantle fluids were closely related to the structural geology of the study area. However, ^{3}H tracer data, estimated mean ages, and the spatial distribution of $\delta^{18}O$ values (Solder and Beisner 2020) and mean age suggest the conceptual model of recharge needs refinement. Namely a second distinct recharge source needs to be considered.

Modern groundwater captured at South Rim springs characterized by ^{3}H greater than ~0.5 TU, suggest a second source of recharge. Possible sources of modern recharge are (1) low-elevation infiltration of run-off through channel bottoms, and (2) plateau recharge transported through structural features to the Redwall-Muav aquifer. The low elevation run-off source of modern recharge is characterized by high recharge temperatures and excess air values and relatively low fractions of winter recharge suggesting infiltration of summer run-off as the likely mechanism. This modern end-member was identified in springs located in alluvium near the mouth of large surface-water drainages. The plateau source of modern recharge has cool recharge temperatures and large fraction of winter precipitation. Spatial patterns of mean age of the regional groundwater indicate relatively consistent groundwater velocities, making fast flowpaths from the high elevations of the southern portion of the study area to be an unlikely source of modern water. A more localized recharge source is further supported by increasing mean age and decreasing fractions of winter recharge from east to west along the South Rim. The eastern portions of the Coconino Plateau are suggested as a recharge source. Previous investigations have not placed much credence in low elevation infiltration and plateau recharge as significant recharge sources, influenced in part by limited data, but more-so on the expectation that presumed high evapotranspiration rates would prevent most of the plateau precipitation from recharging the groundwater system. Investigations of large run-off events in arid regions suggest that a significant portion (up to 50%) of the run-off infiltrates the bed sediment (Vivoni et al.2005; Newman et al. 2006; Meredith et al. 2015; Yang 2017). Semi-quantitative observations (USDA 1986) indicate large run-off infiltration events occur on the South Rim. For plateau recharge, the source was largely dismissed on the basis of groundwater $\delta^{2}H$ and $\delta^{18}O$ values. However, a new interpretation of the data suggests that similarity to winter precipitation does not rule out plateau recharge (Solder and Beisner 2020). Recent findings also suggest plants transpire from a less mobile soil-water reservoir (Evaristo et al. 2015), suggesting infiltrated water is not entirely intercepted by ET but rather likely goes on to become recharge.

Groundwater chemistry not characterized by either modern recharge or the regional groundwater is likely explained by a mixture of the two end-members. Furthermore, local variations in spring chemistry indicate that structural geology is a primary control on the relative contributions of modern and regional groundwater. The results of this study further corroborate already established controls of groundwater flow paths and occurrence of South Rim springs (Huntoon 1977, 2000; Brown and Moran 1979) and Sr isotopic ratios indicating capture of deep (i.e., more radiogenic) flow paths (Monroe et al. 2005) by structural features. As an example from this study, Indian Garden Spring located along the Bright Angel fault has a considerably older age, larger amount of terrigenic-He, and a larger fraction of winter precipitation (i.e., larger fraction of regional groundwater) than the immediately adjacent Horn Creek and Pipe springs. The clear connection between not only occurrence but chemistry and recharge source of groundwater with structural geology provides another important tool for identifying specific springs and recharge points most likely to be affected by change.

A more generalized finding of this study shows that estimated mean ages are less sensitive to variability in assumed aquifer dimensions than variability in tracer concentrations. The implication being conceptual flow model selection is less important than high quality data collection and improved understanding of groundwater flow system transience. Future work toward improving estimates of groundwater age and age distributions would be best served by the collection of additional tracers from established and additional locations (springs and wells). Unfortunately, collection of chlorofluorocarbons and sulphur hexafluoride for this study showed these tracers do not appear promising for age dating South Rim groundwater and there are limited tracer options for such remote sampling. As such, future efforts toward carefully designed campaigns are suggested for investigating seasonal or longer-term variations, if any, in spring chemistry using already proven tracers (i.e., δ^2H, δ^{18}O, ^{3}H, ^{14}C). Although there is an apparent variation in ^{3}H and ^{14}C through time at a given site observed in this data set, the irregular sampling intervals, collection methods, and analytical techniques make temporal analysis of the current data set difficult. Specifically addressing the questions of the presence and magnitude of seasonal variations would be critically important to guide later commitment to long-term data collection.

This new conceptualization of the South Rim flow system has important and immediately relevant implications for protection of groundwater resources. South Rim springs can be differentiated between those capturing entirely young water with high ^{3}H and modern ^{14}C (~100 pmc) and springs that capture some mixture of young and old water, in both cases indicating a connection between the shallow aquifer(s) and the deeper regional system. It is suggested that groundwater mean age and flow paths captured at springs might be reasonably explained by the relative contribution from these two end-members and might then help quantify the vulnerability of a particular spring to hydraulic changes (i.e., groundwater pumping) and contamination. Springs with a large fraction of modern groundwater or recharge from summer precipitation are likely more vulnerable to reductions in recharge rates or contamination introduced by climate change and human activities on the Coconino Plateau (e.g., groundwater extraction, mining, land-use). An identified gap in the current understanding is the temporal variability of spring recharge sources and discharge chemistry. Results from investigation of δ^2H and δ^{18}O (Solder and Beisner 2020) indicate long-term recharge sources are relatively stable on decadal to centurial scale, while the temporal variability in age tracers at select springs indicate recharge source and flow paths are less stable on shorter time periods.

The results of this study indicate a more complex model of recharge to South Rim springs and provide a preliminary measure of spring vulnerability. Continued investigation will be essential for refining the areas where mining activity poses the greatest risk of contamination or where groundwater withdrawals may capture groundwater that would otherwise discharge at these springs along the South Rim of Grand Canyon. Current resource protection strategies may be overly broad in geographic scope and potential impacts may be too uncertain for decision makers to adequately protect the economically, culturally, and ecologically important water resources in the Grand Canyon region from degradation and depletion.

Acknowledgements Thanks go to the USGS Arizona Water Science Center, USGS New Mexico Water Science Center, USGS Grand Canyon Monitoring and Research Center, and Grand Canyon National Park staff for their assistance with sample collection, travel, and logistics. A great many thanks go to the editorial and production staff at *Hydrogeology Journal*. Thanks go to USGS colleague reviewers and the anonymous journal reviewers for their constructive input. Special thanks go to Paula Cutillo and Vic Heilweil for identifying the need for this work and gathering support and to Joel Unema for invaluable field assistance.

Funding information This work was supported by the National Park Service Water Resources Division and the US Geological Survey Toxic Substance Hydrology Program. Any use of trade, firm, or product names is for descriptive purposes only and does not imply endorsement by the US Government.

References

Aeschbach-Hertig W, Peeters F, Beyerle U, Kipfer R (2000) Palaeotemperature reconstruction from noble gases in ground water taking into account equilibration with entrapped air. Nature. https://doi.org/10.1038/35016542

Aeschbach-Hertig W, El-Gamal H, Wieser M, Palcsu L (2008) Modeling excess air and degassing in groundwater by equilibrium partitioning with a gas phase. Water Resour Res https://doi.org/10.1029/2007WR006454

Alpine AE (ed) (2010) Hydrological, geological, and biological site characterization of breccia pipe uranium deposits in northern Arizona. US Geol Surv Sci Invest Rep 2010-5025. https://doi.org/10.3133/sir20105025

Andrews JN (1985) The isotopic composition of radiogenic helium and its use to study groundwater movement in confined aquifers. Chem Geol. https://doi.org/10.1016/0009-2541(85)90166-4

Ballentine CJ, O'Nions RK, Oxburgh ER, Horvath F, Deak J (1991) Rare gas constraints on hydrocarbon accumulation, crustal degassing and groundwater flow in the Pannonian Basin. Earth Planet Sci Lett. https://doi.org/10.1016/0012-821X(91)90133-3

Beisner KR, Tillman FD (2018) Assessing temporal changes in geochemistry at spring sites located in an area of breccia pipe uranium deposits. Geological Society of America Joint Rocky Mountain and Cordilleran Section Meeting Abstracts with Programs, Flagstaff, AZ. https://doi.org/10.1130/abs/2018RM-314266

Beisner KR, Paretti NV, Tillman FD, Naftz DL, Bills DJ, Walton-Day K, Gallegos TJ (2017a) Geochemistry and hydrology of perched groundwater springs: assessing elevated uranium concentrations at Pigeon Spring relative to nearby Pigeon Mine, Arizona (USA). Hydrogeol J. https://doi.org/10.1007/s10040-016-1494-8

Beisner KR, Tillman FD, Anderson JR, Antweiler RC, Bills DJ (2017b) Geochemical characterization of groundwater discharging from springs north of the Grand Canyon, Arizona, 2009–2016. US Geol Surv Sci Invest Rep 2017-5068. https://doi.org/10.3133/sir20175068.

Beisner KR, Solder JE, Tillman FD, Anderson JR, Antweiler RC (2020) Geochemical characterization of groundwater evolution south of Grand Canyon, Arizona (USA). Hydrogeol J. https://doi.org/10.1007/s10040-020-02192-0

Billingsley GH, Hampton HM (2000) Geologic map of the Grand Canyon 30' × 60' quadrangle, Coconino and Mohave counties, northwestern Arizona. US Geol Surv Geol Invest Ser Map I-2688

Billingsley GH, Felger TJ, Priest SS (2006) Geologic map of the Valle 30′ × 60′ quadrangle, Coconino County, northern Arizona. US Geol Surv Sci Invest Map SIM-2895

Billingsley GH, Priest SS, Felger TJ (2007) Geologic map of the Cameron 30′ × 60′ quadrangle, Coconino County, northern Arizona. US Geol Surv Sci Invest Map SIM-2977

Bills DJ, Flynn ME, Monroe SA (2007) Hydrogeology of the Coconino Plateau and adjacent areas, Coconino and Yavapai counties, Arizona. US Geol Surv Sci Invest Rep 2005-5222. https://doi.org/10.3133/sir20055222

Bourg IC, Sposito G (2008) Isotopic fractionation of noble gases by diffusion in liquid water: Molecular dynamics simulations and hydrologic applications. Geochim Cosmochim Acta. https://doi.org/10.1016/j.gca.2008.02.012

Brown BT, Moran MS (1979) An inventory of surface water resources in Grand Canyon National Park, Arizona. Final report, October 1979, Part I of the 208 Water Quality Project, Division of Resource Management, Grand Canyon National Park, Grand Canyon, AZ

Castro MC, Jambon A, de Marsily G, Schlosser P (1998) Noble gases as natural tracers of water circulation in the Paris Basin: 1. measurements and discussion of their origin and mechanisms of vertical transport in the basin. Water Resour Res. https://doi.org/10.1029/98WR01956

Cooley ME (1976) Spring flow from pre-Pennsylvanian rocks in the southwestern part of the Navajo Indian Reservation, Arizona. US Geol Surv Open-File Rep 521-F

Clark IF, Fritz PP (1997) Environmental isotopes in hydrogeology. Lewis, New York

Crossey LJ, Fischer TB, Patchett PJ, Karlstrom KE, Hilton DR, Newell DL, Huntoon P, Reynolds AC (2006) Dissected hydrologic system at the Grand Canyon: interaction between deeply derived fluids and plateau aquifer waters in modern springs and travertine. Geology. https://doi.org/10.1130/G22057.1

Crossey LJ, Karlstrom KE, Springer AE, Newell D, Hilton DR, Fischer T (2009) Degassing of mantle-derived CO2 and He from springs in the southern Colorado Plateau region: neotectonic connections and implications for groundwater systems. GSA Bull. https://doi.org/10.1130/B26394.1

Errol L. Montgomery and Associates (1999) Supplemental assessment of hydrogeologic conditions and potential effects of proposed groundwater withdrawal Coconino Plateau Groundwater Sub-basin, Coconino County, Arizona June 1999. Appendix of Final Environmental Impact Statement for Tusayan Growth, Kaibab National Forest, Williams, AZ, 256 pp Evaristo J, Jasechko S, McDonnell JJ, (2015) Global separation of plant transpiration from groundwater and streamflow. Nature 525 (7567):91-94. https://doi.org/10.1038/nature14983

Farnsworth RK, Thompson ES, Peck EL (1982) Evaporation atlas for the contiguous 48 United States. US National Oceanographic and Atmospheric Administration technical report NWS 33, Washington, DC

Gardner PM, Heilweil VM (2014) A multiple-tracer approach to understanding regional groundwater flow in the Snake Valley area of the eastern Great Basin, USA. Appl Geochem. https://doi.org/10.1016/j.apgeochem.2014.02.010

Gautheron C, Moreira M (2002) Helium signature of the subcontinental lithospheric mantle. Earth Planet Sci Lett. https://doi.org/10.1016/S0012-821X(02)00563-0

Gibs J, Wilde FD, Heckathorn HA (2012) Use of multiparameter instruments for routine field measurements. US Geol Surv Tech Water Resour Invest 9-A6.8. https://doi.org/10.3133/twri09A6.8. Accessed 30 March 2020

Han LF, Plummer LN (2013) Revision of Fontes & Garnier's model for the initial 14C content of dissolved inorganic carbon used in groundwater dating. Chem Geol. https://doi.org/10.1016/j.chemgeo.2013.05.011

Han LF, Plummer LN, Aggarwal P (2012) A graphical method to evaluate predominant geochemical processes occurring in groundwater systems for radiocarbon dating. Chem Geol. https://doi.org/10.1016/j.chemgeo.2012.05.004

Han LF, Roller-Lutz Z, Hunjak T, Lutz HO, Maysumoto T, Aggarwal P (2017) Groundwater response to recharge in the Gacka Area, Croatia, as revealed by stable isotopes, tritium, CFCs and noble gas. Geochem J. https://doi.org/10.2343/geochemj.2.0440

Hart RJ, Ward JJ, Bills, DJ, Flynn ME (2002) Generalized hydrogeology and ground-water budget for the C aquifer, Little Colorado River Basin and parts of the Verde and Salt River Basins, Arizona and New Mexico. US Geol Surv Water Resour Invest Rep 02-4026

Haynes DD, Hackman RJ (1978) Geology, structure, and uranium deposits of the Marble Canyon 1 degree × 2 degrees quadrangle, Arizona. US Geol Surv Miscell Invest Ser Map I-1003

Heaton THE, Vogel JC (1981) "Excess air" in groundwater. J Hydrol. https://doi.org/10.1016/0022-1694(81)90070-6

Hereford R, Bennett GE, Fairley HC (2014) Precipitation variability of the Grand Canyon region, 1893 through 2009, and its implications for studying effects of gullying of Holocene terraces and associated archeological sites in Grand Canyon, Arizona. US Geol Surv Open-File Rep 2014-1006. https://doi.org/10.3133/ofr20141006

Hunt CB (1967) Physiography of the United States. Freeman, New York

Huntoon PW (1977) Relationship of tectonic structure to aquifer mechanics in the western Grand Canyon district, Arizona. Completion report of Project B-31-WYO (14-34-0001-6134) to Office of Water Research and Technology. Water Resources Series no. 66, Water Resources Institute, Washington, DC

Huntoon PW (2000) Variability of karstic permeability between unconfined and confined aquifers, Grand Canyon region Arizona. Environ Eng Sci 6(2):155–170

Huth TE, Cerling TE, Marchetti DW, Bowling DR, Ellwein AL, Passey BH (2019) Seasonal bias in soil carbonate formation and its implications for interpreting high-resolution paleocarchives: evidence from southern Utah. JGR Biogeosci. https://doi.org/10.1029/2018JG004496

Jung M, Aeschbach W (2018) A new software tool for the analysis of noble gas data sets from (ground)water. Environ Modell Softw. https://doi.org/10.1016/j.envsoft.2018.02.004

Jurgens BC, Böhlke JK, Eberts SM (2012) TracerLPM (Version 1): an Excel® workbook for interpreting groundwater age distributions from environmental tracer data. US Geol Surv Tech Methods Rep 4-F3

Kaandorp V, Louw PGB, Velde Y, Broers HP (2018) Transient groundwater travel time distributions and age-ranked storage–discharge relationships of three lowland catchments. Water Resour Res. https://doi.org/10.1029/2017WR022461

Land L, Huff GF (2010) Multi-tracer investigation of groundwater residence time in a karstic aquifer: Bitter Lakes National Wildlife Refuge, New Mexico, USA. Hydrogeol J. https://doi.org/10.1007/s10040-009-0522-3

Land L, Timmons S (2016) Evaluation of groundwater residence time in a high mountain aquifer system (Sacramento Mountains, USA): insights gained from use of multiple environmental tracers. Hydrogeol J. https://doi.org/10.1007/s10040-016-1400-4

Lerback JC, Hynek SA, Bowen BB, Bradbury CD, Solomon DK, Fernadez DP (2019) Springwater provenance and flowpath evaluation in Blue Lake, Bonneville basin, Utah. Chem Geol https://doi.org/10.1016/j.chemgeo.2019.119280

MacDonald GM, Stahle DW, Diaz JV, Beer N, Busby SJ, Cerano-Paredes J, Cole JE, Cook ER, Endfield G, Gutierrez-Garcia G, Hall B, Magan V, Meko DM, Méndez-Pérez M, Sauchyn DJ, Watson E, Woodhouse CA (2008) Climate warming and 21st century drought in southwestern North America. Eos. https://doi.org/10.1029/2008EO090003

McCabe GJ, Palecki MA, Betancourt JL (2004) Pacific and Atlantic Ocean influences on multidecadal drought frequency in the United States. PNAS. https://doi.org/10.1073/pnas.0306738101

Manning AH, Solomon DK (2003) Using noble gases to investigate mountain-front recharge. J Hydrol. https://doi.org/10.1016/S0022-1694(03)00043-X

Meredith KT, Hollins SE, Hughes CE, Cendón DI, Chisari R, Griffiths A, Crawford J (2015) Evaporation and concentration gradients created by episodic river recharge in a semi-arid zone aquifer: Insights from Cl−, δ18O, δ2H, and 3H. J. Hydro. 529:1070-1078. https://doi.org/10.1016/j.jhydrol.2015.09.025

Metzger DG (1961) Geology in relation to availability of water along the South Rim, Grand Canyon National Park, Arizona. US Geol Surv Water Suppl Pap 1475-C

Michel RL, Jurgens BJ, Young MB (2018) Tritium deposition in precipitation in the United States, 1953–2012. US Geol Surv Sci Invest Rep 2018-5086. https://doi.org/10.3133/sir20185086

Monroe SA, Antweiler RC, Hart RJ, Taylor HE, Truini M, Rihs JR, Felger TJ (2005) Chemical characteristics of ground-water discharge at selected springs, South Rim Grand Canyon, Arizona. US Geol Surv Sci Invest Rep 04-5146

Morgan P, Sass JH, Duffield W, Fleger T, Fry BN (2004) Final report to the Department of Energy: Geothermal Resource Evaluation Program of the eastern San Francisco Volcanic Field, Arizona. http://jan.ucc.nau.edu/~pm8/PM_dwnld/SanFranciscoGeothermalFinalReport.pdf. Accessed 8 August 2018

Muller AB, Mayo AL (1986) ^{13}C variation in limestone on an aquifer-wide scale and its effects on groundwater 14C dating models. Radiocarbon 28(3):1041–1054

Mamyrin BA, Tolstikhin IN (1984) Helium isotopes in nature. In: Developments in Geochemistry, vol 3. Elsevier, Amsterdam

National Oceanic and Atmospheric Association (2018) National climatic database. https://ncdc.noaa.gov/cdo-web. Accessed 15 June 2018

National Park Service (2018) NPS stats: National Park Service visitor use statistics. https://irma.nps.gov/Stats/. Accessed 14 August 2018

Newman BD, Vivoni ER, Groffman AR, (2006) Surface water–groundwater interactions in semiarid drainages of the American southwest. Hydrological Processes 20 (15):3371-3394. https://doi.org/10.1002/hyp.6336

Pangle LA, Kim M, Cardoso C, Lora M, Meira Neto AA, Volkmann THM, Wang Y, Troch PA, Harman CJ (2017) The mechanistic basis for storage-dependent age distributions of water discharged from an experimental hillslope. Water Resour Res https://doi.org/10.1002/2016WR019901

Plummer LN, Busby JF, Lee RW, Hanshaw BB (1990) Geochemical modeling of the Madison aquifer in parts of Montana, Wyoming, and South Dakota. Water Resour Res 26(9):1981–2014

Radtke DB, Horowitz AJ, Gibs J, Wilde FD (2002) Raw samples. US Geol Surv Tech Water Resour Invest 9-A5. https://doi.org/10.3133/twri09A5. Accessed 30 March 2020

Reimer PJ, Bard E, Bayliss A, Beck JW, Blackwell PG, Bronk Ramsey C, Buck CE, Cheng H, Edwards RL, Friedrich M, Grootes PM, Guilderson TP, Haflidason H, Hajdas I, Hatté C, Heaton TJ, Hoffmann DL, Hogg AG, Hughen KA, Kaiser KF, Kromer B, Manning SW, Niu M, Reimer RW, Richards DA, Scott EM, Southon JR, Staff RA, Turney CSM, van der Plicht J (2013) IntCal13 and Marine13 radiocarbon age calibration curves 0–50, 000 years cal BP. Radiocarbon. https://doi.org/10.2458/azu_js_rc.55.16947

Ritz GF, Collins JA (2008) pH 6.4 (ver. 2.0, October 2008), US Geol Surv Tech Water Resour Invest 9-A6.4. https://doi.org/10.3133/twri09A6.4. Accessed 30 March 2020

Rounds SA, Wilde FD (2012) Alkalinity and acid neutralizing capacity (ver. 4.0, September 2012). US Geol Surv Tech Water Resour Invest 9-A6.6. https://doi.org/10.3133/twri09A6.6

Rounds SA, Wilde FD, Ritz GF (2013) Dissolved oxygen (ver. 3.0), US Geol Surv Tech Water Resour Invest 9-A6.2. https://doi.org/10.3133/twri09A6.2

Saltzman MR (2002) Carbon and oxygen isotope stratigraphy of the Lower Mississippian (Kinderhookian–lower Osagean), western United States: implications for seawater chemistry and glaciation. GSA Bull 114(1):96–108

Sass JH, Stone C, Bills DJ (1982) Shallow subsurface temperatures and some estimates of heat flow from the Colorado Plateau of northeastern Arizona. US Geol Surv Open-File Rep OF 82-0994

Skrobialowski SC (2016) Capsule- and disk-filter procedure. US Geol Surv Tech Water Resour Invest 9-A5.2.1. https://pubs.usgs.gov/twri/twri9a5/twri9a5_5.2.1.A.pdf. Accessed 30 March 2020

Solder JE (2020) Noble gas isotopes and lumped parameter model results for environmental tracer based groundwater ages, South Rim Grand Canyon, Arizona, USA. US Geol Surv data release. US Geological Survey, Reston, VA. https://doi.org/10.5066/P9WX8N0L

Solder JE, Beisner KR (2020) Critical evaluation of stable isotope mixing end-members for estimating groundwater recharge sources: case study from the South Rim of the Grand Canyon, Arizona, USA. Hydrogeol J. https://doi.org/10.1007/s10040-020-02194-y

Solomon DK (2000) ^{4}He in groundwater. In: Cook PG, Herczeg AL (eds) Environmental tracers in subsurface hydrology. Kluwer, Boston

Solomon DK, Cook PG (2000) ^{3}H and ^{3}He. In: Cook PG, Herczeg AL (eds) Environmental tracers in subsurface hydrology. Kluwer, Boston

Stevens LE, Meretsky VJ (eds) (2008) Aridland Springs in North America: ecology and conservation. University of Arizona, Tuscon, AZ

Stute M, Sonntag C, Deák J, Schlosser P (1992) Helium in deep circulating groundwater in the Great Hungarian Plain: flow dynamics and crustal and mantle helium fluxes. Geochim Cosmochim Acta. https://doi.org/10.1016/0016-7037(92)90329-H

Sullivan S (2018) 2017 Backcountry and river use statistics, Grand Canyon Backcountry Information Center. https://www.nps.gov/grca/planyourvisit/upload/Backcountry_and_River_Use_Statistics_2017.pdf. Accessed 10 January 2018.

Tobin BW, Springer E, Kreamer DK, Schenk E (2017) Review: The distribution, flow, and quality of Grand Canyon Springs, Arizona (USA). Hydrogeol J. https://doi.org/10.1007/s10040-017-1688-8

US Department of Agriculture (1986) Final environmental impact statement canyon uranium mining proposal, Coconino County, Arizona. US Forest Service, Kaibab National Forest, Williams, AZ. https://www.fs.usda.gov/Internet/FSE_DOCUMENTS/stelprdb5346657.pdf. Accessed 12 August 2018

US Geological Survey (2006) Collection of water samples (ver. 2.0). US Geol Surv Tech Water Resour Invest 9-A4. https://doi.org/10.3133/twri09A4. Accessed 30 March 2020

US Geological Survey (2016) USGS National Elevation Dataset (NED) 1 arc-second Downloadable Data Collection from The National Map 3D Elevation Program (3DEP): National Geospatial Data Asset (NGDA) National Elevation Data Set (NED). US Geological Survey, Reston, VA

US Geological Survey (2019a) National Water Information System. US Geol Surv web interface. https://doi.org/10.5066/F7P55KJN

US Geological Survey (2019b) Specific conductance. US Geol Surv Tech Methods 9-A6.3. https://doi.org/10.3133/tm9A6.3

Vivoni ER, Bowman RS, Wyckoff RL, Jakubowski RT, Richards KE, (2006) Analysis of a monsoon flood event in an ephemeral tributary and its downstream hydrologic effects. Water Resources Research 42 (3). https://doi.org/10.1029/2005WR004036

Western Regional Climate Center (2018) SOD USA climate archive: Arizona. Western Regional Climate Center. http://www.wrcc.dri.edu/summary/Climsmaz.html. Accessed March 2018

Wilde FD (ed) (2002) Processing of water samples. US Geol Surv Tech Water Resour Invest 9-A5. http://pubs.water.usgs.gov/twri09A5. Accessed 30 March 2020

Wilde FD (ed) (2004) Cleaning of equipment for water sampling (ver 2.0). US Geol Surv Tech Water Resour Invest 9-A3. http://pubs.water.usgs.gov/twri09A3. Accessed 30 March 2020

Wilde FD (2006) Temperature. US Geol Surv Tech Water Resour Invest 9-6.1. https://doi.org/10.3133/twri09A6.1

Wilde FD, Sandstrom MW, Skrobialowski SC (2014) Selection of equipment for water sampling (ver. 3.1). US Geol Surv Tech Water Resour Invest 9-A2. https://doi.org/10.3133/twri09A2

Yang L, Smith J, Baeck ML, Morin E, Goodrich DC (2017) Flash Flooding in Arid/Semiarid Regions: Dissecting the Hydrometeorology and Hydrology of the 19 August 2014 Storm and Flood Hydroclimatology in Arizona. Journal of Hydrometeorology 18 (12):3103-3123. https://doi.org/10.1175/JHM-D-17-0089.1